AD-775 328

RESEARCH ON MOLECULAR LASERS

George J. Wolga, et al

Cornell University

RESEARCH ON MOLECULAR LASERS

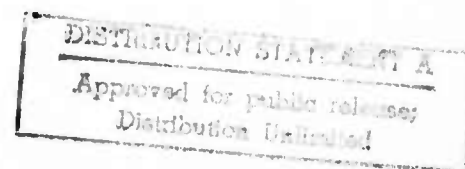ANNUAL REPORT

1 November, 1973

Cornell University

Ithaca, New York 14850

Sponsored by:

Advanced Research Projects Agency

ARPA Order No. 660

ANNUAL REPORT

Reporting Period

1 October 1972 -- 30 September 1973

1.	ARPA Order	660
2.	Program Code Number	0173-7-006252
3.	Name of Contractor	Cornell University
4.	Effective Date of Contract	1 October 1968
5.	Contract Expiration Date	30 September 1973
6.	Amount of Contract for Current Period	$190,000
7.	Contract Number	N00014-67-A-0077-0006
8.	Principal Investigator	Professor G. J. Wolga
9.	Telephone Number	(607)256-3962
10.	Project Scientists	Professor S. H. Bauer (607)256-4028
		Professor T. A. Cool (607)256-4191
		Professor R. A. McFarlane (607)256-4075
11.	Title of Work	RESEARCH ON MOLECULAR LASERS

Sponsored by

ADVANCED RESEARCH PROJECTS AGENCY
ARPA Order No. 660

DOCUMENT CONTROL DATA - R&D

(Security classification of title, body of abstract and indexing annotation must be entered when the overall report is classified)

1. ORIGINATING ACTIVITY (Corporate author)	2a. REPORT SECURITY CLASSIFICATION
Cornell University	Unclassified
Ithaca, NY 14850	2b GROUP N/A

3 REPORT TITLE

STUDY OF MOLECULAR LASERS

4. DESCRIPTIVE NOTES (Type of report and inclusive dates)

Annual Report - 1973

5. AUTHOR(S) (Last name, first name, initial)

George J. Wolga   Ross A. McFarlane
Simon H. Bauer   T. A. Cool

6. REPORT DATE	7a. TOTAL NO. OF PAGES	7b. NO. OF REFS
November, 1973	~~75~~ 83	31

8a. CONTRACT OR GRANT NO.	9a. ORIGINATOR'S REPORT NUMBER(S)
N00014-67-A-0077-0006 b. PROJECT NO.	N/A
c.	9b. OTHER REPORT NO(S) (Any other numbers that may be assigned this report)
d.	N/A

10. AVAILABILITY/LIMITATION NOTICES

11. SUPPLEMENTARY NOTES	12. SPONSORING MILITARY ACTIVITY
	Office of Naval Research

13. ABSTRACT

Research concerning molecular and chemical lasers was conducted in the following areas:

1.   Measurement of $V \rightarrow V$ and $V \rightarrow R, T$ rates among hydrogen halide molecules and the temperature dependence of the energy transfer rates previously determined for HF, DF, HF/CO_2, DF/CO_2 Systems.

2.   Vibrational relaxation studies of $CO_2(00°1)$ in the pressure range 1-100 atm.

3. a.   Chemical laser studies of the reaction of atomic oxygen and acetylene.
    b.   Computer modeling of the $CS_2 - O_2$ chemical laser system.
    c.   Chemical laser studies of the reaction of C_3O_2 with oxygen.

4.   Experimental study of the relaxation of $CO_2(001)$ and $HF(v = 1)$ by collisions with H and F atoms.

5.   Studies of the influence of vibrational excitations on the reaction rate of atom exchange reactions e.g., $HF(v) + D_2 \rightarrow HD + DF$.

DD ~~FORM 1 JAN 64~~ 1473

14.		LINK A		LINK B		LINK C	
KEY WORDS		ROLE	WT	ROLE	WT	ROLE	WT
Molecular Lasers							
Chemical Lasers							
Vibrational Relaxation							
Energy Transfer							
Chemical Reaction Rates							
Vibrational Energy Transfer							

INSTRUCTIONS

1. ORIGINATING ACTIVITY: Enter the name and address of the contractor, subcontractor, grantee, Department of Defense activity or other organization (corporate author) issuing the report.

2a. REPORT SECURITY CLASSIFICATION: Enter the overall security classification of the report. Indicate whether "Restricted Data" is included. Marking is to be in accordance with appropriate security regulations.

2b. GROUP: Automatic downgrading is specified in DoD Directive 5200.10 and Armed Forces Industrial Manual. Enter the group number. Also, when applicable, show that optional markings have been used for Group 3 and Group 4 as authorized.

3. REPORT TITLE: Enter the complete report title in all capital letters. Titles in all cases should be unclassified. If a meaningful title cannot be selected without classification, show title classification in all capitals in parenthesis immediately following the title.

4. DESCRIPTIVE NOTES: If appropriate, enter the type of report, e.g., interim, progress, summary, annual, or final. Give the inclusive dates when a specific reporting period is covered.

5. AUTHOR(S): Enter the name(s) of author(s) as shown on or in the report. Enter last name, first name, middle initial. If military, show rank and branch of service. The name of the principal author is an absolute minimum requirement.

6. REPORT DATE: Enter the date of the report as day, month, year; or month, year. If more than one date appears on the report, use date of publication.

7a. TOTAL NUMBER OF PAGES: The total page count should follow normal pagination procedures, i.e., enter the number of pages containing information.

7b. NUMBER OF REFERENCES: Enter the total number of references cited in the report.

8a. CONTRACT OR GRANT NUMBER: If appropriate, enter the applicable number of the contract or grant under which the report was written.

8b, 8c, & 8d. PROJECT NUMBER: Enter the appropriate military department identification, such as project number, subproject number, system numbers, task number, etc.

9a. ORIGINATOR'S REPORT NUMBER(S): Enter the official report number by which the document will be identified and controlled by the originating activity. This number must be unique to this report.

9b. OTHER REPORT NUMBER(S): If the report has been assigned any other report numbers (either by the originator or by the sponsor), also enter this number(s).

10. AVAILABILITY/LIMITATION NOTICES: Enter any limitations on further dissemination of the report, other than those imposed by security classification, using standard statements such as:

  (1) "Qualified requesters may obtain copies of this report from DDC."

  (2) "Foreign announcement and dissemination of this report by DDC is not authorized."

  (3) "U. S. Government agencies may obtain copies of this report directly from DDC. Other qualified DDC users shall request through

                                                    ."

  (4) "U. S. military agencies may obtain copies of this report directly from DDC. Other qualified users shall request through

                                                    ."

  (5) "All distribution of this report is controlled. Qualified DDC users shall request through

                                                    ."

If the report has been furnished to the Office of Technical Services, Department of Commerce, for sale to the public, indicate this fact and enter the price, if known.

11. SUPPLEMENTARY NOTES: Use for additional explanatory notes.

12. SPONSORING MILITARY ACTIVITY: Enter the name of the departmental project office or laboratory sponsoring (paying for) the research and development. Include address.

13. ABSTRACT: Enter an abstract giving a brief and factual summary of the document indicative of the report, even though it may also appear elsewhere in the body of the technical report. If additional space is required, a continuation sheet shall be attached.

It is highly desirable that the abstract of classified reports be unclassified. Each paragraph of the abstract shall end with an indication of the military security classification of the information in the paragraph, represented as (TS), (S), (C), or (U).

There is no limitation on the length of the abstract. However, the suggested length is from 150 to 225 words.

14. KEY WORDS: Key words are technically meaningful terms or short phrases that characterize a report and may be used as index entries for cataloging the report. Key words must be selected so that no security classification is required. Identifiers, such as equipment model designation, trade name, military project code name, geographic location, may be used as key words but will be followed by an indication of technical context. The assignment of links, roles, and weights is optional.
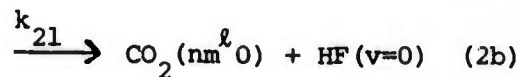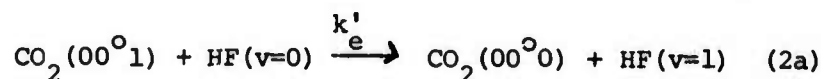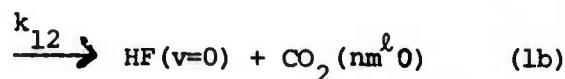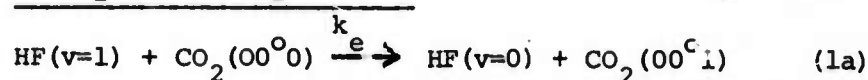
1.   "Temperature Dependence of Vibrational Relaxation

in the HF, DF, HF-CO_2 and DF-CO_2 Systems"

The laser excited fluorescence method has been employed to
determine rate constants for $V \rightarrow V, R$ and $V \rightarrow R, T$ relaxations of HF($v=1$)
and DF($v=1$) by HF, DF, and CO_2 over the range from 295 to $670^{O}K$.

These rate constants exhibit a marked decrease with increasing
temperature. The results provide additional evidence for the conversion
of the large vibrational energy defects of the present systems into
rotational motion of the hydrogen halide under the influence of a size-
able attractive intermolecular potential well.

The measured rate constants and their dependence on temper-
ature are summarized in Tables I and II and Figures 1-3. This work has
been accepted for publication in the Journal of Chemical Physics
(Refs. 3,6). The rate constants and probabilities refer to the processes:

A.   HF-CO_2 and DF-CO_2 Systems:

$$HF(v=1) + CO_2(00^{O}0) \xrightarrow{k_e} HF(v=0) + CO_2(00^{c}1) \qquad (1a)$$

$$\xrightarrow{k_{12}} HF(v=0) + CO_2(nm^{\ell}0) \qquad (1b)$$

$$CO_2(00^{O}1) + HF(v=0) \xrightarrow{k'_e} CO_2(00^{O}0) + HF(v=1) \qquad (2a)$$

$$\xrightarrow{k_{21}} CO_2(nm^{\ell}0) + HF(v=0) \qquad (2b)$$

B. <u>HF and DF Systems</u>:

$$HF(v=1) + DF(v=0) \xrightarrow{k_{12}} HF(v=0) + DF(v=0) \qquad (3a)$$

$$\xrightarrow{k_e} HF(v=0) + DF(v=1) \qquad (3b)$$

$$HF(v=1) + HF(v=0) \xrightarrow{k_{11}} 2HF(v=0) \qquad (4)$$

$$DF(v=1) + HF(v=0) \xrightarrow{k_{21}} DF(v=0) + HF(v=0) \qquad (5a)$$

$$\xrightarrow{k'_e} DF(v=0) + HF(v=1) \qquad (5b)$$

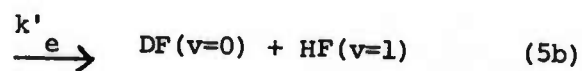$$DF(v=1) + DF(v=0) \xrightarrow{k_{22}} 2DF(v=0) \qquad (6)$$

6
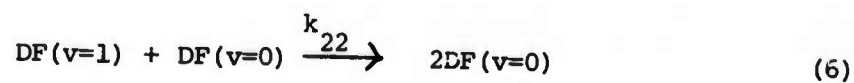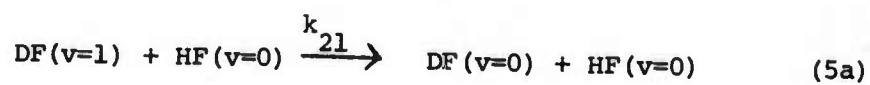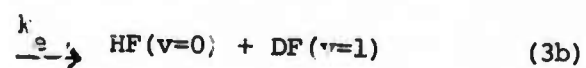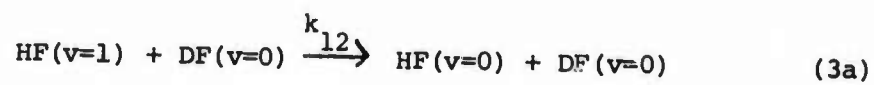
TABLE I

Rate Constant Measurements for HF-CO_2 and DF-CO_2 Mixtures

System	Temperature (°K)	k_{11}	P_{11}	$k_e + k_{12}$	$P_e + P_{12}$	k_{21}	P_{21}
DF-CO_2	299	2.7 ± 0.3	.0038	24.0 ± 5	.030	2.6 ± 0.5	.0032
DF-CO_2[b]	325	2.1 ± 0.3	.0030	19.0 ± 3	.024	2.2 ± 0.3	.0028
DF-CO_2	350	2.0 ± 0.2	.0030	17.2 ± 2.5	.024	1.9 ± 0.4	.0025
DF-CO_2	399	1.2 ± 0.3	.0019	14.6 ± 2.5	.021	1.5 ± 0.4	.0021
DF-CO_2	473	0.87 ± 0.2	.0015	11.7 ± 2.5	.018	1.2 ± 0.3	.0019
DF-CO_2	566	0.77 ± 0.15	.0015	9.7 ± 2.0	.016	1.0 ± 0.2	.0017
DF-CO_2	670	0.64 ± 0.14	.0013	8.6 ± 1.5	.016	0.8 ± 0.2	.0015
HF-CO_2	295	8.4 ± 0.7	.0117	7.0 ± 0.5	.0085	4.7 ± 0.5	.0057
HF-CO_2	324	6.7 ± 0.4	.0098	5.0 ± 0.4	.0062	3.7 ± 0.5	.0047
HF-CO_2[b]	350	5.2 ± 0.3	.0078	3.6 ± 0.3	.0047	3.5 ± 0.5	.0046
HF-CO_2	420	3.9 ± 0.4	.0066	3.1 ± 0.3	.0044	2.7 ± 0.4	.0039
HF-CO_2	500	2.8 ± 0.4	.0053	2.2 ± 0.3	.0035	2.0 ± 0.4	.0031
HF-CO_2	580	2.4 ± 0.4	.0049	2.0 ± 0.3	.0034	1.4 ± 0.3	.0024
HF-CO_2	670	2.0 ± 0.4	.0044	1.8 ± 0.3	.0034	1.1 ± 0.2	.0020

Rate Constants (10^4 sec^{-1} torr^{-1}), and Probabilities[a]

a. The probabilities, P have been calculated from the relationship $P = 4k/n\bar{v}\pi(d_1 + d_2)^2$, where d_1 and d_2 are the molecular diameters; k is the measured rate constant (sec^{-1} · torr^{-1}); n is the number density of molecules (cm^{-3} · torr^{-1}); and $\bar{v}$ is the average speed of approach between molecules of a given pair. For HF and DF a collision diameter of 3.0 Å has been assumed; collision diameters of 3.3 Å have been taken for HCl and DCl, and a value of 3.9 Å has been taken for CO_2, see J. O. Hershfelder, C. F. Curtis and R. B. Bird, Molecular Theory of Gases and Liquids (Wiley, New York, 1954), pp. 597, 1200.

b. See reference (3).

TABLE II

Rate Constant Measurements for Mixtures of HF and DF

Temperature	Rate Constants (10^4 sec^{-1} Torr^{-1})			
	k_{11}	$k_e + k_{12}$	k_{22}	$k_e' + k_{21} \approx k_{21}$
297	8.4 ± 1.0	13.5 ± 1.0	2.5 ± 0.4	4.1 ± 0.4
321	7.1 ± 0.5	11.0 ± 0.8	1.9 ± 0.4	3.4 ± 0.4
395	4.3 ± 0.5	7.3 ± 0.5	1.0 ± 0.3	2.3 ± 0.3
475	2.7 ± 0.3	5.1 ± 0.3	0.8 ± 0.1	1.5 ± 0.2
570	2.1 ± 0.3	3.9 ± 0.4	0.5 ± 0.2	1.2 ± 0.2
678	2.0 ± 0.3	3.2 ± 0.3	0.5 ± 0.2	0.9 ± 0.2

REFERENCES

1. R. R. Stephens and T. A. Cool, J. Chem. Phys. $\underline{56}$, 5863 (1972).

2. J. L. Ahl and T. A. Cool, J. Chem. Phys. $\underline{58}$, 5540 (1973.

3. R. A. Lucht and T. A. Cool, "Temperature Dependence of Vibrational Relaxation in the HF, DF, $HF-CO_2$, and $DF-CO_2$ Systems", J. Chem. Phys. to be published.

4. J. C. Stephenson, J. Finzi and C. B. Moore, J. Chem. Phys $\underline{56}$, 5214 (1972).

5. T. A. Dillon and J. C. Stephenson, J. Chem. Phys. $\underline{58}$, 2056 (1973).

6. R. A. Lucht and T. A. Cool, "Vibrational Relaxation in HF and DF Mixtures",J. Chem. Phys. to be published.

9

FIGURE CAPTIONS

FIGURE 1

Temperature dependences for the probabilities for the energy transfer processes of Equations (3) → (6). The probabilities, P, have been calculated as discussed in reference (3): Δ, Ref. 1; $\blacktriangle$, Ref. 2; $\bullet$, Ref. 3; o, present work.

FIGURE 2

Comparison of the temperature dependences of the V → V, R transfer probabilities for process (1a) for the $HCl-CO_2$, $DCl-CO_2$, $HF-CO_2$ and $DF-CO_2$ systems: Δ, $HCl-CO_2$, Stephenson, et al., ref. 4; $\blacktriangle$, $DCl-CO_2$, Stephenson, et al., ref 4; $\Diamond$, $HCl-CO_2$, theory of Dillon and Stephenson, ref 5; $\Box$, $HF-CO_2$, Stephens and Cool, Ref. 1; O, $HF-CO_2$, present work; O, $HF-CO_2$, theory of Dillon and Stephenson, Ref. 5; $\blacksquare$, $DF-CO_2$, Stephens and Cool, ref. 1; $\bullet$, $DF-CO_2$, present work; $\blacklozenge$, $DF-CO_2$, theory of Dillon and Stephenson, ref. 5.

FIGURE 3

Comparison of the temperature dependences of the V → R, T deactivation probabilities of $CO_2(00^{\circ}1)$ molecules by process (2b) for HCl, DCl, HF and DF: Δ, CO_2-HCl, Stephenson, et al., ref 4; $\blacktriangle$, CO_2-DCl, Stephenson, et al., ref. 4; $\Box$, CO_2-HF, Stephens and Cool, ref. 1; O, CO_2-HF, present work; $\blacksquare$, CO_2-DF, Stephens and Cool, ref. 1; $\bullet$, CO_2-DF, present work.

FIGURE I

FIGURE 2

FIGURE 2

$HX(\upsilon=1) + CO_2(00°0) \longrightarrow HX(\upsilon=0) + CO_2(00°1)$

DF - CO₂

HCl - CO₂

HF - CO₂

DCl - CO₂

PROBABILITY

TEMPERATURE (°K)

12

FIGURE 3

$$CO_2(00^\circ1) + HX \longrightarrow CO_2(nm'o) + HX$$

CO_2-HF

CO_2-DF

CO_2-DCl

CO_2-HCl

PROBABILITY

TEMPERATURE (°K)
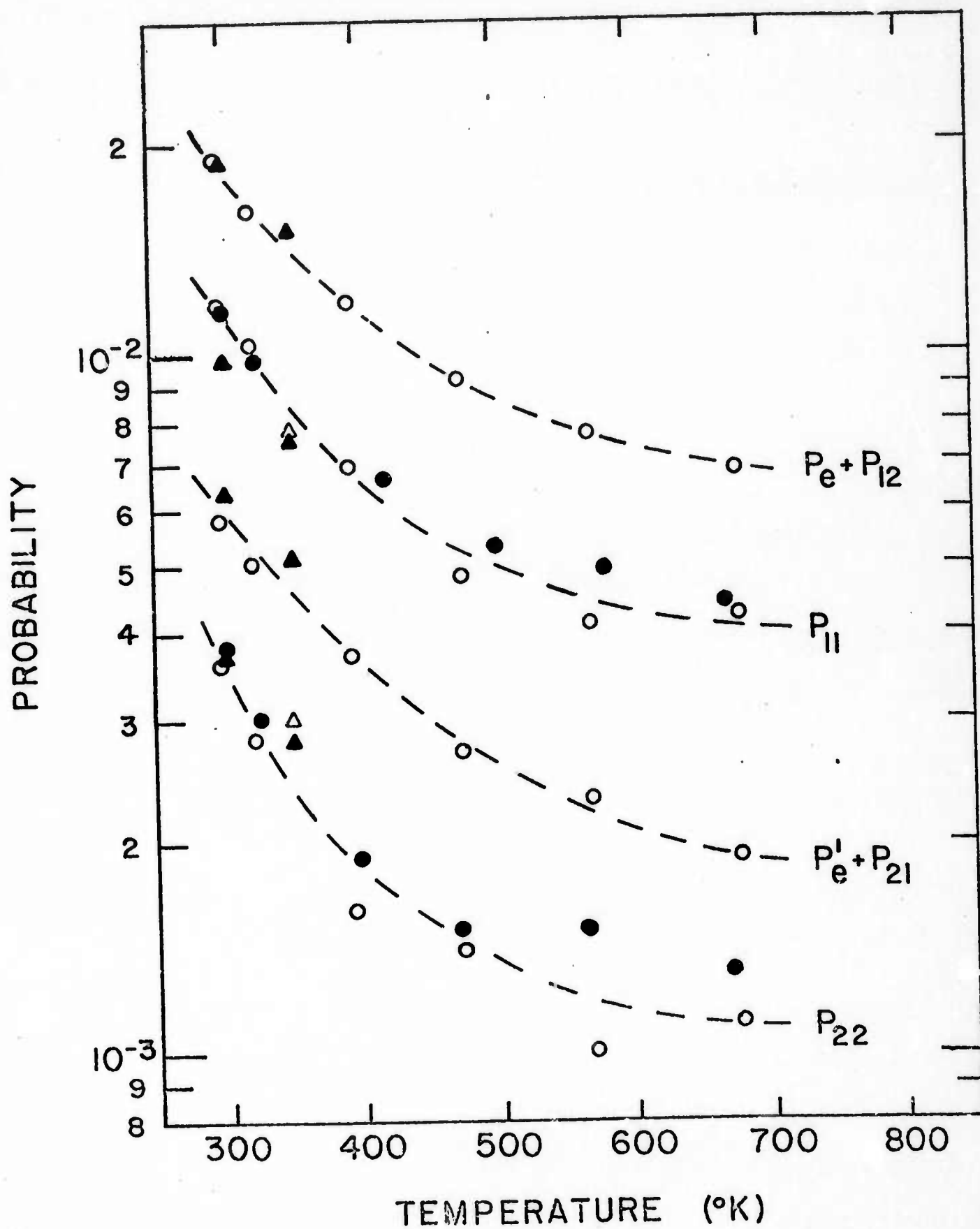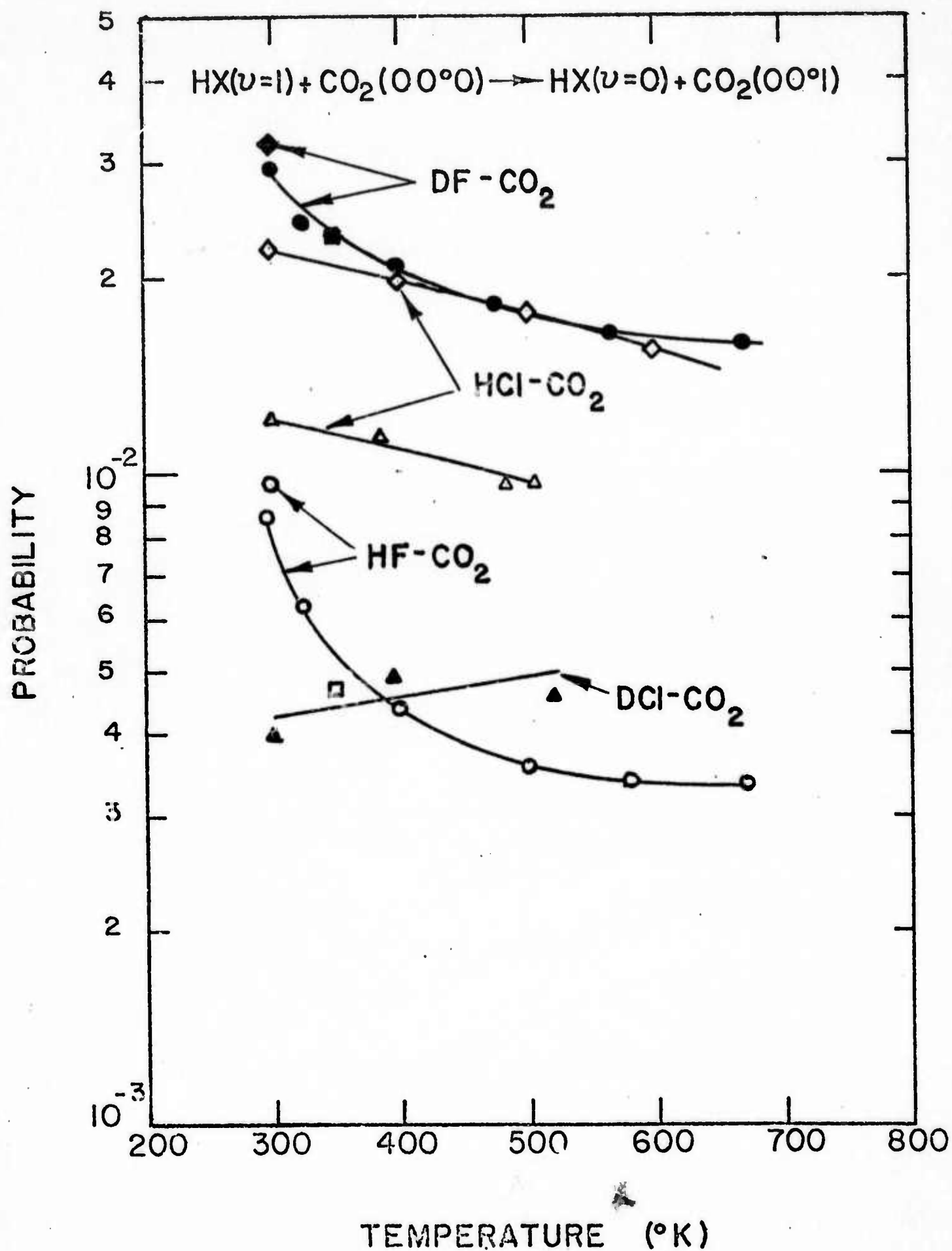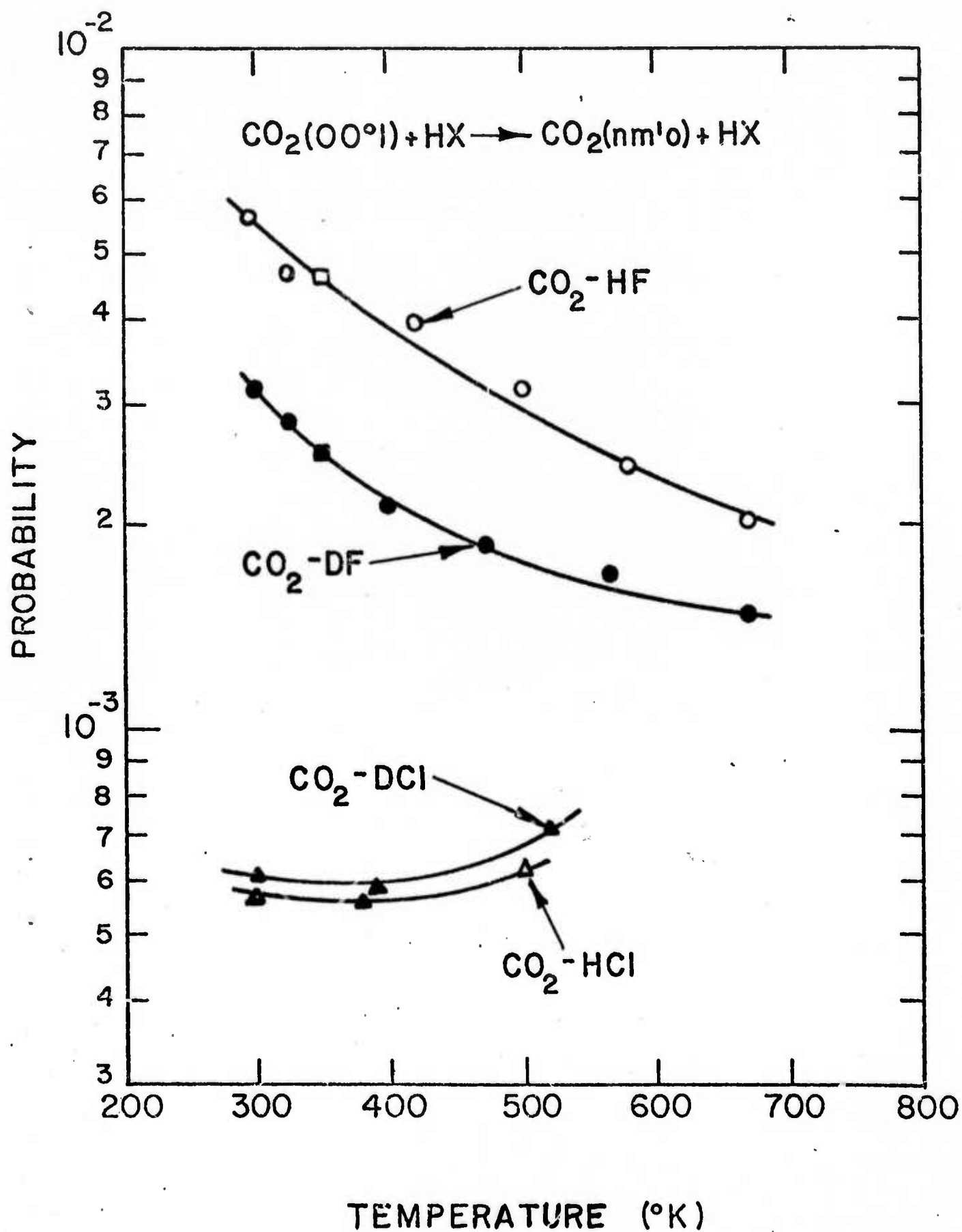
2.

High Pressure Vibrational Relaxation of the $(00°1)$ State of CO_2

Professor G. J. Wolga

The need for good experimental data concerning the vibrational relaxation time of $CO_2(00°1)$ at high pressures due to self collisions and collisions with N_2, He and other molecules is evident from two considerations.

1. High pressure CO_2 lasers already operate at pressures exceeding one atmosphere and have been proposed by many investigators at much higher pressures as well. The motivation to operate at high pressure is, of course, to increase the density of energy storage and to increase laser power.

2. Very little is known concerning CO_2 relaxation above one atmosphere and, in fact, there is little other data to use for guessing or extrapolating to high pressures.

Data from ultrasonic measurements exists for the ν_2 mode at or slightly above room temperature and over the pressure range 10 - 750 atm. Measurements of ν_3 relaxation over a wide temperature range exist for low pressures. Fig. 2 shows the domain of prior measurements and the range of this work. High pressure measurements of ν_3 relaxation simply do not exist. To complicate matters, the critical point of CO_2 occurs at about $310°K$ and 80 atm. CO_2 lasers have been considered for this region of pressure and temperature and it is not clear whether any unusual relaxation behavior can be expected at or near the critical point. The current investigation was planned to provide experimental data in the range $100°K < T < 400°K$ and $1 \text{ atm} < p < 500 \text{ atm}$.

14-

Because the $CO_2(00\overset{\bullet}{}1)$ relaxation rate is expected to increase at least proportionally with pressure we anticipated the requirement to measure very short relaxation times. It was concluded that conventional time resolved laser induced fluorescence would be impractical over the planned range of experimental pressures. An experimental method was therefore devised in which time integrated fluorescence signals could be compared.

With reference to Fig. 2, a measurement of the total energy absorbed E_a at $4.3\,\mu$ by CO_2 in the transition $CO_2(00\overset{\bullet}{}0) \rightarrow CO_2(00\overset{\bullet}{}1)$ is measured using detectors D_2 and D_3. The time integrated fluorescence power at $10.6\,\mu$, E_f, due to the transition $CO_2(00\overset{\bullet}{}1) \rightarrow CO_2(10\overset{\bullet}{}0)$ is measured by detector D_1. If we refer measurements at (p, T, x_j) to those taken under standard conditions $(p^{(0)}, T^{(0)}, x_j^{(0)})$ where x_j are sample mole fractions then it is shown in the Appendix that if the collisional decay of $CO_2(00\overset{\bullet}{}1)$ population is described by a single exponential decay with decay constant k_d that:

$$\frac{k_d^{(0)}}{k_d(p,T)} = \frac{E_f(p,T)}{E_f^0} \cdot \frac{E_a^{(0)}}{E_a(p,T)} \cdot \frac{A^{(0)}}{A(p,T)}$$

where A is the Einstein spontaneous emission coefficient and the assumption is made that the fluorescence signal detected is a fixed proportion of the total fluorescence energy. Therefore, the high pressure measurements need not be time resolved and can be simply related to measurements under some standard condition, e.g. $p = .1$ atm, $T = 300\overset{\bullet}{}K$ where k_d is known from laser induced fluorescence experiments. It should be noted that if the Einstein coefficient proves to be strongly pressure dependent it will have to be obtained by independent experiments or calculated.

We have performed measurements at $296°K$ over the pressure range 1 - 5 atm for pure CO_2. We find

$$k_d(296°K, \; 40 \; psia) = 2.0 \pm 0.2 \; k_d(296°K, \; 20 \; psia)$$

$$k_d(296°K, \; 75 \; psia) = 2.3 \pm 0.2 \; k_d(296°K, \; 40 \; psia)$$

Thus no significant departure from linearity appears over this pressure range and laser performance can be scaled using low pressure rates safely to 5 atm. We shall report on higher pressure measurements when they are completed.

16

Appendix

Fluorescence Ratio Technique - Derivation

Let: E_a = energy absorbed from laser beam at frequency ν_a

$h\nu_a = E(00^\bullet 1) - E(00^\bullet 0)$

N_a = No. of laser photons absorbed = $\dfrac{E_a}{h\nu_a}$

E_f = total fluorescence energy emitted at frequence ν_f

$h\nu_f = E(00^\bullet 1) - E(10^\bullet 0)$

N_f = # fluorescence photons emitted = $\dfrac{E_f}{h\nu_f}$

A_f = A - coef. for fluorescence at ν_f

$p(t)$ = probability that a molecule put in state $|u\rangle$, the state of
interest, at time $t = 0$ will be in $|u\rangle$ at time t. Note
$p(0) \equiv 1$, and $p(t)$ is proportional to the decay curve of
fluorescence as usually observed.

The probability/unit time that an excited molecule will fluoresce
is A_f.

For small probabilities, the probability that a molecule excited
to $|u\rangle$ at $t = 0$ will emit a fluorescence photon in $(t, t+dt)$ is given by
$A_f p(t)\,dt$.

Thus, the probability that a molecule initially excited to $|u\rangle$ will
ever fluoresce is:

$$\int_0^\infty A_f\, p(t)\, dt \quad .$$

If energy E_a was absorbed from the laser beam $N_a = \dfrac{E_a}{h\nu_a}$ molecules
were initially in $|u\rangle$ but

N_f = No. fluorescence photons = (No. initially in $|u\rangle$) x

(prob that a molecule initially in $|u\rangle$ will emit)

17-

$$\therefore \quad N_f = \frac{E_f}{hV_f} = \left(\frac{E_a}{h\nu_a}\right) \times \left(\int_0^\infty A_f \, p(t) \, dt\right)$$

Since A is not a function of time, we can rearrange this as follows:

$$\int_0^\infty p(t) \, dt = \frac{1}{A_f}\left(\frac{\nu_a}{\nu_f}\right)\left(\frac{E_f}{E_a}\right) \qquad \text{--- (1)}$$

Let the superscript (0) denote a reference state: $p^{(0)}, T^{(0)}, x_i^{(0)}, \ldots$ where the x_i and the mole fractions of the various species.

Write (1) for an arbitrary state and (0) for the reference state; divide the two equations to get

$$\frac{\int_0^\infty p(p; pT, x_i, \ldots) \, dt}{\int_0^\infty p(t; p^{(0)}, T^{(0)}, x_i^{(0)}, \ldots) \, dt} = \frac{A(p^{(0)}, T^{(0)}, x_i^{(0)}, \ldots)}{A(p, T, x_i, \ldots)} \cdot \frac{E_f(p, T, x_i, \ldots)}{E_f(p^{(0)}, T^{(0)}, x_i^{(0)}, \ldots)} \cdot$$

$$\frac{E_a(p^{(0)}, \ldots)}{E_a(p, T, \ldots)}$$

$$\text{--- (2)}$$

To use this equation, it is assumed that the integrated fluorescence signal as seen by the fluorescence detector is always a fixed proportion of the total fluorescence energy.

Special cases:

1. Single exponential decay: $\quad p(t) = e^{-k_d t}$

$$\int_0^\infty p(t) \, dt = \frac{1}{k_d}$$

$$\therefore \quad \frac{k_d^{(0)}}{k_d} = \left(\frac{E_f}{E_f^{(0)}}\right)\left(\frac{E_a^{(0)}}{E_a}\right)\left(\frac{A^{(0)}}{A}\right) \qquad \text{---- (3)}$$

18—

It should be noted that the decay of $|u\rangle$ can be due to collisions with the same species or with another species as long as the decay is single exponential. The reference state can be either the mixture or else pure CO_2.

19-

New Laser System Studies $C_2H_2 + O$
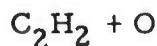
We have been exploring the reaction of atomic oxygen with acetylene as a means to provide vibrationally excited CO molecules with a distribution of population appropriate for producing optical gain and laser oscillation near 5 microns wavelength. Previous reports have discussed the development of a microwave excitation source for producing large flow rates of atomic oxygen and the studies of spontaneous emission from the CO formed in the reactions

$$O + C_2H_2 \rightarrow CO + CH_2 + 51 \text{ Kcal./mole} \tag{1}$$

$$O + CH_2 \rightarrow CO + 2H + 71 \text{ K cal./mole} \tag{2}$$
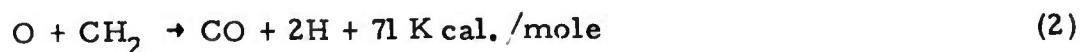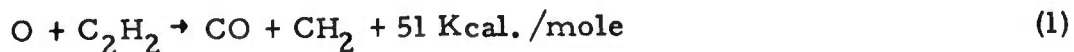
The exothermicity of these reactions makes available sufficient energy for excitation of CO molecules to $v' = 13$ and collisional V-V energy exchange permits the development of significant populations at even higher vibrational levels.

For laser purposes the central question concerns the relative distribution of the chemically formed CO molecules over the vibrational levels and whether sufficiently high local vibrational temperatures can be achieved (or negative temperatures) to provide either a partial or total population inversion.

Our last report discussed experimental determinations of the relative population distribution by means of observations of the spontaneous emission from excited CO species on overtone transitions from 2.3 μ to 3.0 μ wavelength. By means of a computer simulation technique which

uses relative vibrational populations and rotational temperature as input parameters to synthesize a spectrum which matches the one observed it was possible to establish the relative populations from $v' = 2$ to $v' = 14$ under various operating conditions of pressure, fuel flow rate and additive gases.

This work established that at relatively low production rates of CO^* species, a vibrational temperature of $8000\,°K$ described the observed population distribution. Significant modification of this distribution occurs at higher CO concentrations with the effects of Treanor pumping becoming very evident. Higher vibrational levels exhibited local vibrational temperatures of $14,000\,°K$ comparable to those found in electrically excited CO lasers while the local temperature for levels $v = 2$ to $v = 4$ approached $3000\,°K$ as is consistent with Treanor's theory.

More significantly however our observations were extended to include the effect of cold $CO(v = 0)$ added to the fuel to provide a preferential relaxation of low vibrational levels. Using a "fast-flow" approximation, the analysis of the data permitted a much more direct determination of the rates of some of the operative V-V relaxation processes. Good agreement was obtained with both our theoretical calculation of these rates as well as measurements made by Hancock and Smith under very different experimental conditions.

It was determined in our measurements that the addition of cold CO could take advantage of the maximum in V-V rates near $v' = 5$ to provide a "total vibrational inversion" between levels $v'' = 5, 6, 7$. This is of course just the requirement for laser emission on transitions $7 \rightarrow 6$ and $6 \rightarrow 5$. A model was set up to represent the time development of <u>all</u> vibrational populations up to $v' = 14$ in a dynamic situation when radiative, V-V and V-T processes were operative and it was possible to simulate

the appearance of the total inversion between levels $v' = 5, 6, 7$ as had been established experimentally. The computer determined time evolution showed the appearance of a total inversion due to all processes can take place in a time $150 - 200\,\mu$ sec. following the start of relaxation.

The computer simultation of the relaxation kinetics is only approximate in that it assumes a number of things not true in the experiment. In particular, no account is taken of the finite mixing time of the acetylene as it is injected into the flowing oxygen stream and further the model starts with an initial CO distribution and does not consider the reaction of $O + C_2H_2$ as it develops in time. Nevertheless both the experimental and theoretical results indicate that the reaction can provide a population distribution appropriate for laser operation. It remains to consider whether the experimental situation of the present experiments is adequate to exploit the reaction in a laser.

This requires an estimate of the actual population densities present in our system for the purpose of calculating a gain coefficient. Using the known densities of the reactants at $t = 0$

$$[C_2H_2]_0 = 0.3 \times 10^{-8} \text{ mole/cm}^3 \tag{3}$$

$$[O]_0 = 1.3 \times 10^{-8} \text{ mole/cm}^3 \tag{4}$$

and using the reported reaction rate constant

$$k = 8 \times 10^{10} \text{ cm}^3 \text{ mole}^{-1} \text{ sec}^{-1} \quad \text{(Stuhl and Niki, J.C.P., } \underline{55}, \text{ 3854,} \tag{5}$$
$$\text{1971.)}$$

determined from vacuum u.v. photolysis, we can write

$$[CO] = [C_2H_2]_0 \{1 - e^{-(k[O]_0 t)}\} \tag{6}$$

In a time $t = 200 \, \mu$ sec approximately 20 per cent of the acetylene will have reacted and the expected CO concentration is

$$[CO] = 5.6 \times 10^{-10} \text{ mole/cm}^3 \tag{7}$$

$$= 3.4 \times 10^{14} \text{ mole/cm}^3 \tag{8}$$

Since relaxation is occurring even as the CO* is being produced this represents only a very crude estimate of the total CO concentration. From the observed population ratios, our experimental conditions therefore represent populations.

$$N_7 \simeq 1.5 \times 10^{13} \text{ molecules/cm}^3$$

$$N_6 \simeq 1.4 \times 10^{13} \text{ molecules/cm}^3 \tag{9}$$

$$N_5 \simeq 1.2 \times 10^{13} \text{ molecules/cm}^3$$

The gain coefficient can be written

$$\alpha = \frac{8\pi^3 c}{3kT} \left(\frac{M}{2\pi kT} \right)^{1/2} |R_0|^2 \, vJ$$

$$\cdot \left\{ B_{v'} N_{v'} e^{-F_v(J-1)hc/RT} - B_{v''} N_{v''} e^{-F_{v''}(J)hc/RT} \right\} \tag{10}$$

For a rotational temperature of $300\,^\circ$K, introducing our above estimates for the $P_{6 \to 5}(10)$ transition which is the transition for maximum gain we estimate

$$\alpha(P_{6 \to 5}[10]) = 1.8 \times 10^{-3} \text{ cm}^{-1} \tag{11}$$

and for the $7 \to 6$ transition

$$\alpha(P_{7 \to 6}[10]) = 1.2 \times 10^{-3} \text{ cm}^{-1} \tag{12}$$

In the longitudinal flow system the overall gain length is not well defined. Our computer simulation shows gain developing over several hundred microseconds. With a flow velocity of 80 m/sec. and $t \cong 500\ \mu$ sec. our active length is approximately 4 cms. and our maximum gain is

$$P_{6-5}(10) \qquad G = e^{\alpha L} = e^{4 \times 1.8 \times 10^{-3}} = 1.007 \qquad (13)$$

$$P_{7-6}(10) \qquad G = 1.005$$

As relaxation proceeds in the flow direction the region beyond our reaction zone can be expected to introduce some loss and it is apparent that a transverse geometry is more appropriate.

Nevertheless two experiments were carried out in an attempt to confirm the above gain estimates. The last semi-annual report described a two-beam measurement system which had been set up to provide a normalized differential measurement of gain or loss for a single frequency CO laser propagating along the axis of our flow system and through the reaction zone. The intrinsic noise of the detectors and signal processing electronics indicated that a differential gain or loss of 0.1 per cent should be detectable. During the course of the experiment carried out on

$$P_{7 \to 6}(10) \qquad \lambda = 5.1334\ \mu$$

and

$$P_{6 \to 5}(10) \qquad \lambda = 5.0663\ \mu$$

however, fluctuations in the probe laser power level with possible contributions to noise from gas turbulance and nonuminformities in the region of the gas column in the microwave discharges gave rise to signal fluctuations in excess of 1 per cent and the presence of gain on the single pass transit could not be determined with certainty.

The gains estimated above should be adequate to provide laser oscillation in a system where some care is taken to minimize optical

losses. An optical cavity was set up using opaque gold mirrors. The single Brewster window in the system was a fresh laser quality KCl flat and provided the only output coupling from the cavity. Detection was by means of a gold doped germanium detector. The cavity and the detector were aligned by operating the system at 10.6μ using $CO_2 - N_2$. During operation of the $O + C_2H_2$ reaction the detection sensitivity was adequate to observe spontaneous emission from the reaction zone more than one meter away from the detector. The conditions of gas discharge, fuel, oxygen and cold CO known to produce the total inversion discussed above were reproduced but no laser oscillation was observed. Changes in gas composition in an effort to increase the CO^* production rate were unsuccessful in obtaining oscillation. These final experiments were carried out using an increased pumping capacity which would be expected to increase the gain length L but it was still not possible to reach oscillation threshold in the longitudinal flow system. A flow velocity of 192 m/sec. was obtained which would provide a gain region of approximately 10 cm.

25

Chemical Laser Studies

$\underline{C_3O_2 + O_2}$ Chemical Laser

During the past year we engaged in three projects. The major
effort was directed to the study of CO lasing from the $C_3O_2 + O_2$ + He
system. When mixtures of these reagents are subjected to a brief
electrical (initiating) pulse (5 nf, ≈ 10 Kv, ≈ 1 µs duration) various
radiations are emitted in the following sequence (depending in detail
on the specific composition and voltages used): visible and UV, mostly
from C_2 ($A^3\pi$), starts at about 3 µs, peaks at 15 µs and dies down slowly
at about 100 µs; in the absence of a laser cavity, chemiluminescence in
the IR from excited CO vibrational states ($V' = 16 \rightarrow 2$) can be detected
at 35 µs, peaks at ≈ 200 µs and thereafter decreases slowly; in an
appropriately aligned cavity, CO lasing starts at about 300 µs, peaks
at 1 ms, and lasts for about 2 ms. A complete report of this study is
attached.

A complete literature survey of all the reactions that we can
conceive as operating in this mixture was undertaken. The complete
set were then analyzed, and the important reactions were incorporated
in a general kinetics program which include:

1. all chemical production steps, and their inverses;

2. computation of the appropriate thermodynamic functions and
   rate parameters as dependent on the temperature, when a
   suitable set of parameters is inserted for each component.

3. computation of the system temperature for adiabatic
   conditions.

4. v-T and v-v relaxation steps.

5. radiative losses.

To date computations indicate that 19 <u>chemical</u> reactions must be included in the program, not counting the two pumping reactions, each of which consists of about 15 steps. We have yet to obtain an adequate match of the distribution of chemiluminescent intensities as observed by Dr. Sheasley. However, it is very clear that both $C_2O + O \rightarrow CO^{\ddagger} + CO$, and $C_3O_2 + O \rightarrow CO^{\ddagger} + 2CO$, contribute to pumping. The present set of reactions and their rate constants are appended in Table I.

27-

3c)

$CS_2 + O_2$ Chemical Laser

Our work in this program during the past year consisted exclusively
of library searches and computations for the $CS_2 + O_2 + He$ system.   A
set of about 70 possible reactions for this mixture was assembled, and by
successive testing all but about 28 were eliminated.   These simulate
the $CS_2 + O_2$ laser data which we obtained during the previous year.
Although a perfect fit of the time evolution of lasing for the various
transitions has not yet been computed, we believe that we are close enough
such that matching will be obtained by making small adjustments in the
kinetics parameters, and changing the assumed magnitudes for the
(initial) composition of reagents produced by the discharge.   Early
difficulties with the computations called to our attention several subtle
aspects of the computer program, and led to rather surprising conclusions
regarding the specific reactions which must be incorporated in order to
generate an internally consistent mechanism.   We are now preparing a
report in which all the significant reactions that were considered are
listed with justification for the selection of their rate constants.   The
basic set of reactions is attached as Table II.

Bending Mode Relaxation in CO_2

We undertook to develop a fluorescence technique for measuring vibrational relaxation times for the (0n0) states of CO_2. Vibration-translation energy transfer efficiencies at ambient temperatures from the bending mode of CO_2 to various collision partners had been limited to two techniques, ultrasonic dispersion and impact-tube pressure decrements; both are difficult to implement. Shock tube data, using the density gradient at the shock front, cannot be extrapolated to lower temperatures without incorporating an assumed temperature dependence for the vibration relaxation time. To resolve this ambiguity we sought a simpler, more reliable and widely applicable technique. The 2.8 micron laser emission from $HF^{\ddagger}$ pumps the $(10^{\bullet}1)$ and $(02^{\bullet}1)$ levels of CO_2. Line center frequency mismatching is rectified partially by pressure broadening with argon, or with mixtures which incorporate the collision partners of interest. At CO_2 concentrations above 2% collisions with the ground state rapidly degrade the pumped states to overpopulate the $(00^{\bullet}1)$ and (0n0) states, from which fluorescence is observed at 4.3 μ and 15 μ, respectively. The decay rates of the latter can be reduced to V-T relaxation times. We are now attempting to resolve the several contributions to 15 μ fluorescence, from the several upper emitting states, by measuring the effect of increasing density of a cold CO_2 filter on the fluorescent radiation intensity and decay time. We are also working with a computer program which permits correlation of the populations in the various fluorescent states with assumed rate constants for V-V transfers and V-T relaxations. The completion of this work will be reported soon.

TABLE I

No.	Reaction	A $cm^3/mol \cdot sec$	E_a (kcal)
1	$C + CO_2 + M \rightarrow CO + CO$	3.0×10^{13}	5.1
2	$C + C_2O \rightarrow C_2 + CO$	6.0×10^{13}	0.6
3	$C + O_2 \rightarrow CO + O$	1.0×10^{14}	2.8
4	$C_2O + O_2 \rightarrow CO + CO_2$	2×10^{12}	1.5
5	$C_2O + O_2 \rightarrow 2CO + O$	2×10^{12}	1.5
6	$C_3O_2 + O \rightarrow C_2O + CO_2$	2.0×10^{12}	2.2
7	$O_3 + M \rightarrow O + O_2 + M$	2.0×10^{15}	24.0
8	$O + O_3 \rightarrow 2O_2$	3.0×10^{13}	6.0
9	$C_2 + O \rightarrow CO + C$	1.0×10^{14}	3.0
26	$CO_2 + C_2 \rightarrow C_2O + CO$	7.0×10^{13}	6.00
27	$C + C_3O_2 \rightarrow 2CO + C_2$	1.0×10^{13}	4.00
28	$C_2O + C_2O \rightarrow 2CO + C_2$	4.0×10^{12}	3.0
29	$C_2O + O \rightarrow C_2 + O_2$	6.0×10^{13}	54.5
30	$C_2O + O \rightarrow CO_2 + C$	2.0×10^{13}	3.6
31	$C + C_2O \rightarrow C_3 + O$	3.0×10^{13}	4.0
32	$C_3 + C \rightarrow C_2 + C_2$	1.0×10^{14}	36.0
33	$C_2 + C_2O \rightarrow CO + C_3$	3.0×10^{13}	0.7
34	$C_3 + O \rightarrow CO + C_2$	6.0×10^{13}	0.7
35	$C_3 + O_2 \rightarrow 2CO + C$	5.0×10^{12}	1.5
10 ↓ 25	$C_2O + O \rightarrow CO^{(0)} + CO^{(0)}$ etc. $\searrow CO^{(15)}$	1.72×10^{13} ⟩ 1.41×10^{12} ↙	0.6 0.6
36 ↓ 47	$C_3O_2 + O \rightarrow CO^{(0)} + 2CO$ etc. $\searrow CO^{(11)}$	8.7×10^{12} ⟩ 9.2×10^{10} ↙	2.0 2.0

$$k = A \exp(-E_a/RT)$$

TABLE II

No.	Reaction	A $cm^3/mol \cdot sec$	E_a (kcal)
1	$O + CS_2 \rightleftharpoons CS + SO$	1.2×10^{13}	1.05
2	$CS + O \rightleftharpoons CO^{(v)} + S$	1×10^{14}	1.5
3	$O + CS_2 \rightleftharpoons S + OCS$	1×10^{14}	10.0
4	$O + OCS \rightleftharpoons SO + CO$	1.9×10^{13}	4.53
5	$O + O_2 + M \rightleftharpoons O_3 + M$	1.34×10^{13}	-2.1
6	$O + O_3 \rightleftharpoons 2 O_2$	1.2×10^{13}	4.79
7	$S + CS_2 + M \rightarrow (CS_3) + M$	3.75×10^{16}	-1.25
8	$(CS_3) + S \rightarrow CS_2 + S_2$	1.2×10^{10}	ratio of reaction rate
9	$(CS_3) + O \rightarrow CS_2 + SO$	2.4×10^{10}	over dissociation
10	$(CS_3) + SO \rightarrow CS_2 + S_2O$	1.2×10^{9}	$CS_3 \rightarrow CS_2 + S$
11	$S + O_2 \rightleftharpoons O + SO$	1×10^{14}	2.58
12	$O + S_2 \rightleftharpoons S + SO$	1.9×10^{13}	1.8
13	$O + SO + M \rightleftharpoons SO_2 + M$	3.2×10^{17}	0
14	$SO + O_3 \rightleftharpoons O_2 + SO_2$	1.5×10^{12}	2.1
15	$SO + O_2 \rightleftharpoons O + SO_2$	2×10^{13}	10.0
16	$SO + SO \rightleftharpoons S + SO_2$	2×10^{13}	10.0
17	$SO + SO \rightarrow (S_2O_2)$	3.2×10^{12}	3.5
18	$(S_2O_2) + CS \rightarrow S_2O + OCS$	1×10^{11}	0
19	$(S_2O_2) + CS \rightarrow CS_2 + SO_2$	1×10^{11}	0
20	$(S_2O_2) + O_2 \rightarrow SO_2 + SO_2$	1×10^{11}	0
21	$(S_2O_2) + O \rightarrow S_2O + O_2$	1×10^{12}	0
22	$(S_2O_2) + O \rightarrow SO + SO_2$	1×10^{12}	0
23	$(S_2O_2) + S \rightarrow SO_2 + S_2$	1×10^{12}	0

TABLE II (Continued)

No.	Reaction	A $cm^3/mol \cdot sec$	E_a (kcal)
24	$(S_2O_2) + SO \rightarrow S_2O + SO_2$	1×10^{11}	0
25	$S_2O + O_2 \rightleftharpoons SO + SO_2$	1×10	0
26	$S_2O + O \rightleftharpoons SO + SO$	1×10^{11}	0
27	$S_2O + O \rightleftharpoons S_2 + O_2$	1×10^{10}	0
28	$S_2O + SO \rightleftharpoons S_2 + SO_2$	1×10^9	0

LASING ACTION AND THE

RELATIVE POPULATIONS OF VIBRATIONALLY EXCITED

CO PRODUCED IN PULSE-DISCHARGED $C_3O_2 + O_2$ + He MIXTURES

D. Sheasley and S. H. Bauer

Department of Chemistry, Cornell University, Ithaca, New York 14850

ABSTRACT

Our studies of the $C_3O_2 + O_2$ + He pulsed laser consist of four parts. First, both literature and experimental surveys were made of preparative methods, in search for an efficient route for generating substantial quantities of the suboxide. In this we were only partially successful. Yields of up to 15% were obtained, compared to conventional yields of about 8%. The second part consisted of a parametric study of reagent composition and of discharge conditions to maximize laser output for an axial discharge configuration, and the recording of relative lasing intensities and delays for onset of lasing as a function of upper vibrational state. The effect of added cold CO was also investigated. In the third part, relative populations of excited states, as present at a sequence of delays after pulse initiation, were obtained from chemiluminescence data, in the absence of lasing. Finally, visible and UV spectra emitted during the induction period for lasing were recorded, and assigned to specific transitions from upper electronic states due to C_2, CO_2 and O_2^+.

INTRODUCTION

In a previous publication from this laboratory[1] we reported the observation of stimulated CO emission from C_3O_2 + O_2 mixtures when initiated by a short high voltage electrical discharge. The radiation intensities were considerably lower than those generated under comparable conditions with CS_2 + O_2 mixtures, even though the net exothermicity for the postulated pumping step is considerably higher for the former than the latter. There are a variety of factors which would favor C_3O_2 as fuel for a lasing system, were it not for its low efficiency. For example, the carbon suboxide oxidation produces practically no net pollutants, and with minimal precautions leads to no explosive mixtures. In contrast, the CS_2 + O_2 combination not only pollutes but presents grave explosive hazards. However, carbon suboxide is difficult to prepare in large quantities and comparatively expensive. In this report we describe the first stage of our study of the mechanism of C_3O_2 + O_2 chemiluminescence when pulse initiated. Our objectives were: (i) to explore the preparative procedures for increasing the efficiency of synthesis at the 10 gram level; (ii) to examine the basis for the low lasing yields obtained thus far, and (iii) to attempt to determine the initial population distribution of the various vibrationally excited states of CO.

REGARDING THE SYNTHESIS OF C_3O_2

Carbon suboxide was first prepared by the dehydration of malonic acid with phosphorous pentoxide using a procedure similar to that described by Miller and Fateley[2]. The major difference in our preparation was that the reaction was carried out at a lower temperature (50-60°C) over a longer period of time (1-2 days). Twenty

grams of malonic acid were mixed with 200 grams/phosphorous pentoxide in a 2-liter round-bottom flask. Occasionally up to 100 gms of dry sea sand were also included. The reactant flask was attached to a vacuum line and heated. The volatile products (carbon suboxide, carbon dioxide, and acetic acid) were collected in a trap cooled with liquid nitrogen. At the end of the heating period the carbon dioxide was removed by pumping on the raw product held at $-117^{\circ}C$ with a bath of liquid-solid ethanol. The carbon suboxide was then distilled from the acetic acid at $-78^{\circ}C$. The purity of the carbon suboxide was checked by vapor pressure measurements and infrared spectra. Yields obtained using this procedure were typically about 8%. Although no quantitative determination of all the reaction products was performed, our observations regarding this preparation concur with the conclusion of Stock and Stoltzenberg[3] that the low yield can be attributed mainly to the polymerization of the carbon suboxide formed, rather than to the competing decomposition into carbon dioxide and acetic acid.

Other reactions and preparative schemes have been proposed and tested for better yields. The following modifications were tried during the course of this study. (i) Malonic acid was added to a slurry formed by the rapid stirring of a mixture of phosphorous pentoxide and mineral oil at $50-60^{\circ}C$. Carbon suboxide yields of less than 5% were obtained using this method. The color of the slurry changed to yellow-gold during the course of the reaction , suggesting that most of the carbon suboxide produced dissolved in the paraffin oil and subsequently polymerized. (ii) The dehydration of malonic acid was carried out with polyphosphoric acid (PPA) in place of the powdered phosphorous pentoxide. Malonic acid was added to PPA at temperatures ranging from room temperature to $100^{\circ}C$. Large quantities of carbon dioxide were collected, but in none of these experiments was any carbon

suboxide obtained. The appearance of a yellow color in the reactant solution indicated that some carbon suboxide had been produced but that it had undergone polymerization before it effervesced from the solution.

(iii) The dehydrohalogenation of malonyl dichloride was tested as a possible synthetic route. Malonyl chloride was added dropwise to a column of basic alumina in vacuo. Large quantities of hydrogen chloride were obtained, but the dehydrohalogenation did not go to completion since no carbon suboxide was obtained. Dehydrohalogenation was also attempted by adding malonyl chloride to tri-butyl amine; again no significant yield the desired product was obtained.

There are reports in the literature on the preparation of carbon suboxide by the pyrolysis of diacetyltartaric anhydride; the most recent is that of Miller and Fateley[2], who obtained a yield of 2%. In 1922, Ott[4] claimed yields of up to 40% using this method. His results, however, are probably in error. It appears that ketene is thus produced in large quantities and it is virtually impossible to separate it from C_3O_2 by subsequent purification procedures. The latter point has also been discussed by Long, Murfin and Williams[5] and by Smith, et.al.[6].

To date we found no synthetic route for carbon suboxide superior to the dry malonic acid-phosphorous pentoxide dehydration reaction. Tests with other solid dehydrating agents (alumina, silica) when used by themselves produced no product; when added to the P_2O_5 always reduced the yield or caused severe caking. We then sought to improve the yield by modifying the experimental conditions. It seemed conceivable that more product would be obtained were the solid reactants continuously stirred or kept thoroughly mixed during the course of the reaction. To minimize "caking", to maintain good contact between the solid reagents and to sweep out the

36-

C_3O_2 as rapidly as it is produced we constructed the reaction vessel pictured schematically in Figure 1a,b,c. It consists of a 3" diameter glass tube which is rotated about a stationary core. The reactor can be evacuated, and the stationary core is equipped with inlet and outlet tubes for the flow of an inert gas. Provision is made for heating the entire assembly.

Rotation of the glass tube continuously mixes the malonic acid and phsophorous pentoxide. As water is picked up by the dehydrating agent, the mixture tends to cake on any surface that is available. An essential feature of the stationary core are the strips of stainless steel which scrape the solid reactants from the walls of the rotating glass tube. The addition of dry sand to the reactant mixture helps significantly to maintain good mixing. Nevertheless, caking cannot be completely avoided, specially on the stainless steel scrapers, thereby inhibiting mixing of the reactants as the reaction progressed.

The usual quantities of reactants used in the reactor just described were 20 gms malonic acid, 200 gms phosphorous pentoxide, and 200-400 gms dry sand. The reactor was heated to a temperature of 35-50°C for 1-2 days while helium flowed at a partial pressure of 10-20 torr. Yields of carbon suboxide were typically 12-15%. The reactant mixture was yellow at the completion of the reaction, indicating that a great deal of polymerization still had occurred. Much less carbon dioxide was produced in this apparatus than in the static dehydration apparatus described earlier, thus making the purification procedure (see Fig. 2) considerably less time consuming. Subsequent to each preparation, the C_3O_2 was distilled into a pyrex trap with a single teflon stopcock. The C_3O_2 could then be stored in a dewar of liquid nitrogen or dry ice-acetone without showing noticeable signs of polymerization.

In the laser experiments   described below carbon suboxide is used in a continuous flow system. Typical operating conditions require maintaining a partial pressure of C_3O_2 of about 0.2 torr. To provide the quantities of C_3O_2 needed for the present laser studies, the malonic acid-phosphorous pentoxide synthesis was run about 50 times.

EXPERIMENTAL ARRANGEMENT

The overall experimental arrangement is essentially the same as that used in our investigation of the $CS_2 + O_2$ system. The laser consists of a 1" I. D. pyrex tube, 1 meter in length, equipped with NaCℓ windows at the Brewster angle. A capacitor is discharged through the flowing gas mixture _via_ two aluminum ring electrodes. The charge on the capacitor (0.005 μf) is released through an ignitron (WL-7703) triggered at 6 Hz. The flow of each component gas is controlled by a fine needle valve, with vernier settings. Pressures in the laser tube is measured with a Wallace and Tiernan diaphragm manometer (0-20 torr).

The laser cavity was set by two gold coated spherical Ge mirrors (4 meter radius) placed 1.5 meters apart. One of the mirrors had an uncoated hole (0.75 mm diameter) in its center for coupling out the laser emission. The emission from the laser cavity passed through an I.R. filter, which has a flat response between 4.1 and 5.6 μ and was monitored by a Au doped Ge detector cooled to 77°K. The output from the detector passed through an FET impedance reducer and was displayed on an oscilloscope (Tektronix 535). The integrated power of the laser emission was measured by passing the vertical signal output from the oscilloscope through a pulse stretcher (Ge diode with a 0.47 μf capacitor) to the input of a lock-in amplifier (PAR Model 120); the reference signal was synchronized with the trigger pulse that initiated the discharge. Some measurements were made of the laser

power by taking the vertical signal output from the oscilloscope to the input of a boxcar integrator (PAR Model 160). Data obtained with the two instruments compared quite satisfactorily.

Dispersed wavelength studies were made with Perkin-Elmer 88G I.R. grating monochromator, equipped with a Bausch and Lomb grating, 150 ℓ/mm and blazed at 6 μ. The monochromator was calibrated by measuring several lines of a low pressure mercury lamp in high orders. The wavelength response of the monochromator and of Au doped Ge detector system was calibrated by recording the emission of a Nernst glower lamp whose temperature was measured with an optical pyrometer, assuming that the emissivity was constant over the 0.65-5 μ region.

The fundamental CO spontaneous emission was measured from one end of the tube with the cavity mirror removed and the Brewster angle window replaced by a window set perpendicular to the axis of the tube. Chemiluminescence from a region close to the end of the tube was then focused onto the slit plane of the monochromator with a spherical mirror, f. ℓ. = 10 cm. Otherwise discharge conditions were the same for laser operation. The output from the monochromator was sampled with the boxcar integrator for a duration of 2.5 μsec using a constant preset delay time after the discharge. The monochromator was scanned over the CO fundamental region, thereby providing the emission spectrum of CO at a given delay time.

Lasing was tested in a pin type discharge. This tube is 2.5" I.D. and 1 meter long. The discharge is imposed transverse to the gas flow through 150 pins plus 1 KΩ resistors connected in parallel. A copper ground strip is located on opposite side of the tube. Discharge conditions in this arrangement differ significantly from those in the axial discharge (ring electrode) laser tube. The optical cavity and the

electronics were the same as described above except that the discharge was controlled by a spark gap rather than an ignitron and larger capacitors (0.01-0.03 μf) were used.

Optimum operating conditions for lasing in the transverse discharge typically required higher gas pressures than in the axial discharge. In the former, the minimum pressure of C_3O_2 to achieve lasing was about 1.5 torr which, under our flow conditions, led to a consumption rate of about 2 g/min. In view of our limited supply of C_3O_2 very few runs were made with the pin discharge unit. The results described below were obtained with the axial discharge laser.

SPECTROSCOPIC MEASUREMENTS

Laser radiation at 5.1-5.5 μm, corresponding to transitions in CO from $v'-v'' = 6-5$ to 11-10, was observed subsequent to a pulsed electrical discharge through gaseous mixtures of carbon suboxide, oxygen, and helium (Table I). The fact that lasing appears only after substantial time delays, and the observation that similar discharge pulses through CO-He or CO-He-O_2 mixtures do not produce stimulated emission indicate that the excitation of CO occurs via chemical reaction rather than electrical excitation of previously generated CO.

The total integrated laser power was studied as a function of the discharge voltage and the partial pressures of the component gases. The dependence of laser power on C_3O_2 pressure for a range of discharge voltages is shown in Figure 3. There is an optimum voltage for maximum laser power in the range 9-15 Kv for each of the three sets of conditions. The maximum shifts toward higher values as the C_3O_2 pressure is increased. It is also evident that for a given pressure of O_2 there is an optimum pressure of C_3O_2; as the O_2 increases, the optimum C_3O_2

concentration also increases.

The effect of the O_2 pressure on laser power is illustrated in Figure 4. Note that the higher the O_2 pressure the lower the optimum voltage. Figure 5 shows the effect of variation in the pressure of the helium diluent. A marked increase in total power is obtained upon increasing the helium pressure from 2.48 to 5.57 torr. This has essentially no effect on the optimum discharge voltage. Lasing could not be achieved in these experiments in the absence of a diluent. It is likely that He is necessary to lower the CO rotational temperature. Pressures of up to 0.2 torr of SF_6, H_2 and N_2O were also added to the C_3O_2-O_2-He mixture. Each of these strongly quench the laser.

No measurements of the absolute power of the C_3O_2-O_2-He laser system were made. However, we compared it with that of CS_2-O_2-He chemical laser, as studied in this laboratory.[7] The power output of the CS_2-O_2-He laser exceeds that of the C_3O_2-O_2-He system under similar discharge and cavity conditions by 2 to 3 orders of magnitude.

The time delay between the discharge and the initiation of the laser pulse depended primarily on the discharge voltage and the C_3O_2 pressure. This is illustrated in Figure 6, in which the delay time is plotted as a function of (a) C_3O_2 pressure and (b) O_2 pressure for 10, 12, and 14 Kv discharges. The (a) data show a marked decrease in the delay time as the C_3O_2 pressure is increased for all three discharge voltages. As can be seen in part (b), the dependence of the delay time on O_2 pressure is complex. The effect for a given discharge voltage, however, is not nearly as significant as changes in C_3O_2 pressure.

Figure 7 shows the effect on the integrated power of cold CO added to the mixture. Small additions increase the laser power slightly, but further additions substantially quench laser oscillations. The discharge voltage for maximum laser power increases

with increasing pressure of added CO. The addition of CO markedly decreased the delay times, as is illustrated in Figure 8 and/Table II. Both the initiation and termination times of the laser pulse are reduced substantially for all the vibrational transitions that participate in the lasing. The addition of 0.97 torr CO to a mixture of 0.19 torr C_3O_2, 0.62 torr O_2, and 3.75 torr He, for example, reduces the delay time by about a factor of 5. The discharge voltage for minimum delay time, however, shows no apparent change as CO is added to the mixture.

Dispersed spectra obtained with the P-E grating monochromator indicated that the laser radiation extended from about 5.1 to 5.5 μm. This interval corresponds to transitions in CO from (v'-v'') = 6-5 to 11-10. Stimulated emission of the 11-10 transition was very weak. The maximum intensity appeared at the 8-7 transition.

Attempts were made to obtain the delay times of individual vibration-rotation transitions using a wavelength controlled cavity. A grating (300 ℓ/mm, Bausch and Lomb, blazed at 3.5 μm) replaced the totally reflecting cavity mirror so that laser oscillations within the cavity could be confined to a single vibration-rotation line, thus eliminating the effects of cascading due to stimulated transitions on the delay times. Unfortunately, the output power using this cavity was generally either too weak to be recorded with our detector, or the lasing threshold was not attained. Occasionally a lasing line was located, but a systematic study could not be performed.

Monochromator scans of the IR chemiluminescence emitted from the discharge tube, in the absence of cavity mirrors, was completed for delay times of 40, 80, 100, 200, and 400 μsec after the discharge pulse. The operating conditions were: 0.19 torr C_3O_2, 0.55 torr O_2, 3.75 torr He, with a 12 Kv discharge. The spectrum thus obtained was analyzed with the aid of a computer program, which has been

described in detail by Tsuchiya, Nielsen and Bauer[7], to determine the relative populations of CO vibrational levels at each delay time. A least squares procedure provided the set of relative vibrational populations which gave the best agreement between the calculated and the observed spectra. The distributions were then graphically smoothed. The rotational temperature of $450^{\circ}K$ used in the calculations was determined from measurement of the rotational temperature of HCl added as a tracer to the discharge. Temperature differences of $\pm 50^{\circ}K$ made only minor differences in the deduced distributions.

The relative populations of CO vibrational levels obtained by this procedure are plotted in Figure 9 and tabulated in Table III. / To facilitate comparison, the results were normalized at $v = 8$. The distribution at 40 μsec is the least reliable set because of the weakness of the emission at that delay time. As is apparent from Figure 9, the distributions at the three earliest time delays are quite similar, exhibiting minima at $v = 5-6$ and 11-12 and maxima at $v = 8$ and 14-15. The distributions at 200 and 400 μsec, depicted in Figure 10, show considerable relaxation. Nevertheless, there persists a noticeable leveling off in the distribution in the $v = 7-10$ region.

To obtain quantitative information regarding the rate of CO production, it is necessary to estimate the population in the $v = 0$ level using a linear extrapolation, a procedure subject to large uncertainties. The populations were then summed for each delay time. The resulting values indicate that the total amount of CO almost attained its maximum value after about 100 μsec. In view of the inverted population obtained from the emission spectra at 100 μsec, one would expect lasing to be initiated sooner than that observed. This difficulty has not yet been resolved.
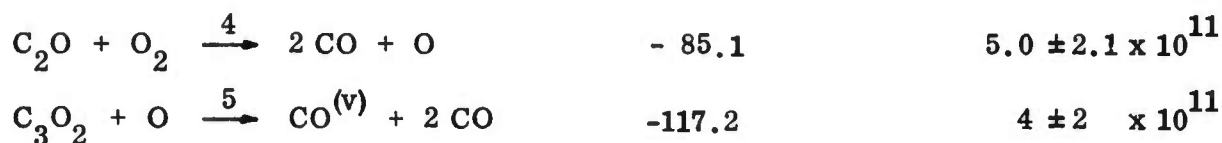
43

The visible and UV radiation emitted from the discharge was also examined. Quartz windows were attached to the discharge tube, and the emission was directed into a Jarrell-Ash $\frac{1}{2}$ meter Ebert-type spectrometer; the detector was a 1P28 photomultiplier. Discharge conditions were the same as for laser operation. By far the most intense feature between 2000 and 6500 Å (Table IV) was the Swan system of C_2 ($A^3\Pi_u$ - $X^3\Pi_g$). Much weaker bands which could be assigned to the high pressure bands and to the Deslandres-d'Azambuja system of C_2 were also observed. The weaker bands which were recorded were assigned to CO_2 and O_2^+. The C_2 emission appeared at 3 μsec after the discharge pulse, rose to a maximum intensity in about 20 μsec, and then decayed gradually, finally disappearing after about 300 μsec.

The dependence of the C_2 emission on operating parameters was studied by monitoring the (0-0) band as the gas mixture and discharge voltage were changed. The intensity of C_2 emission was enhanced by decrease in O_2 pressure, by increasing the C_3O_2 pressure, and by higher discharge voltages. No correlation between C_2 emission and laser power could be established.

COMMENTS ON THE MECHANISM

A tentative mechanism was proposed in our initial report[1]. From the several investigations described in literature[8-12] rate constants[8,9] and exothermicities are available for the following reactions, measured at room temperature (these are subject to revision):

	ΔH^o (kcal/mole)	$k(300^oK)$ $mole^{-1}cm^3sec^{-1}$
$C_3O_2 + O \xrightarrow{1} C_2O + CO_2$	- 40.0	$1 \pm 0.5 \times 10^{10}$
$C_2O + O \xrightarrow{2} CO^{(v)} + CO$	-204.7 (v=0)	$5.7 \begin{smallmatrix} +3.4 \\ -2.2 \end{smallmatrix} \times 10^{13}$
$C_2O + O_2 \xrightarrow{3} CO + CO_2$	-212.7	$4.9 \pm 2.1 \times 10^{11}$

$$C_2O + O_2 \xrightarrow{\;4\;} 2\,CO + O \qquad\qquad -\,85.1 \qquad\qquad 5.0 \pm 2.1 \times 10^{11}$$

$$C_3O_2 + O \xrightarrow{\;5\;} CO^{(v)} + 2\,CO \qquad\qquad -117.2 \qquad\qquad 4 \pm 2 \;\times 10^{11}$$

In the above it is presumed that the oxygen atoms are in their ^3P state. Lin and
Brus[13] reported that the attack of $O(^1D)$ on C_3O_2 _via_ a reaction analogous to (5)
produced stimulated CO emission, and observed transitions $(v'-v'') = 13\text{-}12$ to $5\text{-}4$. In
their case oxygen atoms were generated by flash photolysis (in the vacuum UV) of
SO_2, under conditions where no C_3O_2 decomposition was anticipated. In contrast,
it is likely that the high voltage discharge in the $C_3O_2 + O_2 +$ He mixtures not only
produces atomic oxygen but also fragments the suboxide. This is compatible with
our observation that the total laser power first increased and then decreased when
the discharg d voltage was increased. That the delay for onset of lasing decreased
with increasing C_3O_2 pressure but increased with higher discharged voltages also
suggests that fragmentation of C_3O_2 contributed significantly to laser action. These
arguments point to (2) is the essential step; indeed, it has the largest rate constant
by two orders of magnitude over the others listed above. It is interesting to note
that were the exothermicity of (5) to appear exclusively as vibrational excitation, and
were this equally divided among the three product molecules, each CO could be
excited to the $v = 6$ state. Such a reaction, therefore, might explain the maximum
$v \approx 8$ in the vibrational distribution. Reaction (5) must be considered as a contributing
pumping step. Populations in the higher levels from which lasing is observed can be
easily attained by v-v transfers. The appearance of a second maximum in the
vibrational population at $v \approx 14\text{-}15$ is compatible with the results of Clough, Schwartz,
and Thrush[14] who observed an intensity maximum in the CO overtone emission at
$v = 16$, in the chemiluminescence study of the reaction between C_3O_2 and O atoms.

45

They suggested that this feature it is due to reaction (2).

At this stage it is not evident that a chain reaction can be maintained in this system. Qualitative consideration of the rate constants listed above indicates that this is unlikely, unless one were to postulate augmentation of the pyrolysis of C_3O_2 by the vibrationally excited CO generated via (2) and (5); i.e. that this system operates with an energy chain.

The appearance of strong emission from C_2 ($A^3\Pi_u$) as an afterglow, necessitates the assumption of additional reactions for the pre-lasing induction period. At $400^\circ K$

$$C_2O + O \xrightarrow{\enspace 6 \enspace} C_2 + O_2$$
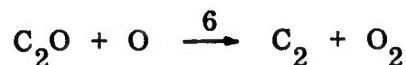
is endothermic by about 72 kcal. Further, it requires 86 kcal to fragment C_2O into CO + C atoms, and an even larger amount to break it apart into C_2 + O fragments. Thus we conclude that carbon atoms are generated (from the suboxide) during the discharge, and these attack C_2O:

$$C + C_2O \xrightarrow{\enspace 7 \enspace} C_2 + CO.$$

While this step is exoergic by 86 kcal and is more than sufficient to excite C_2 to the A state (≈ 55 kcal/mole), we have yet to demonstrate such a chemi-excitation. Collisions with residual electrons would not account for the extended period over which the C_2 emission (maximum at 20 μsec, and decay over ≈ 300 μsec).

ACKNOWLEDGEMENT

REFERENCES

1. M. C. Lin and S. H. Bauer, Chem. Phys. Lett., 7, 223 (1970).

2. F. A. Miller and W. G. Fateley, Spectrochim. Acta, 20, 253 (1964).

3. A. Stock and H. Stoltzenberg, Chem. Ber., 50, 498 (1917).

4. E. Ott, Umschau, 26, 576 (1922).

5. D. A. Long, F. S. Murfin and R. L. Williams, Proc. Roy. Soc. London, 223A, 251 (1954).

6. R. N. Smith, D. A. Young, E. N. Smith and C. C. Carter, Inorg. Chem., 2, 829 (1963).

7. S. Tsuchiya, N. Nielsen and S. H. Bauer, J. Phys. Chem., in press.

8. D. G. Williamson and K. D. Bayes, J. Am. Chem. Soc., 89, 3390 (1967).

9. W. L. Shackleford, F. N. Mastrup and W. C. Kreye, J. Chem. Phys., 57, 3933 (1972).

10. K. H. Becker and K. D. Bayes, J. Chem. Phys., 48, 653 (1968).

11. K. D. Bayes, J. Chem. Phys., 52, 1093 (1970).

12. G. Liuti, C. Kunz and S. Dondes, J. Am. Chem. Soc., 89, 5542 (1967).

13. M. C. Lin and L. E. Brus, J. Chem. Phys., 54, 5423 (1971).

14. P. N. Clough, S. E. Schwartz and B. A. Thrush, Proc. Roy. Soc., London, 317A, 575 (1970).

47

TABLE I. Laser emission from the C_3O_2-O_2-He mixtures. Operating conditions were: P_{He} = 3.83 torr, P_{O_2} = 0.60 torr, $P_{C_3O_2}$ = 0.20 torr; 12 Kv discharge; monochromator slit width = 50 μm.

(v'-v'')	P(J)	delay time (μsec)	Relative Intensity
10-9	P(16)	550	0.5
10-9	P(14)	800	1.0
9.8	P(16)	450	1.2
9-8	P(15)	550	5.8
9-8	P(12)	850	3.0
8-7	P(18)	400	0.6
8-7	P(15)	450	5.0
8-7	P(13)	700	10.0
7-6	P(16)	500	2.0
7-6	P(15)	450	3.5
7-6	P(14)	900	0.2
7-6	P(13)	800	4.0
7-6	P(11)	1100	1.9
7-6	P(10)	1200	1.7
6-5	P(16)	600	1.5
6-5	P(15)	800	1.4

TABLE II. Effect of added CO on emission time for laser oscillations in the C_3O_2-O_2-He system. Operating parameters common to both sets of data are: $P_{He} = 3.79$ torr, $P_{O_2} = 0.65$ torr, $P_{C_3O_2} = 0.18$ torr; 12 Kv discharge; monochromator slit width = 50 μm.

Laser Pulse Duration (μsec) After Initiation

(v'-v")	P(J)	No CO		$P_{CO} = 0.53$ torr	
		Starts	Terminates	Starts	Terminates
10-9	P(16)	500	1200	200	650
10-9	P(15)	600	1300	200	750
9-8	P(15)	500	1400	200	700
9-8	P(12)	1000	1900	400	1200
8-7	P(15)	500	1100	150	650
8-7	P(13)	750	1700	300	850
7-6	P(13)	800	1500	300	800
7-6	P(11)	1200	2200	500	1000

TABLE III

Relative Populations Deduced From Chemiluminescent Intensities

| v	40 μsec	80 μsec	100 μsec	200 μsec	400 μsec
1	(18.88)	(15.00)	(11.06)	(15.00)	(11.00)
2	7.50	5.48	4.78	6.29	6.94
3	3.75	2.96	2.56	4.41	4.03
4	2.00	1.57	0.24	2.41	2.19
5	0.88	0.74	0.09	2.00	1.61
6	1.25	0.30	0.65	1.47	1.22
7	1.13	0.52	0.96	1.00	1.08
8	1.00	1.00	1.00	1.00	1.00
9	1.00	0.83	0.56	1.00	0.89
10	0.38	0.52	0.24	0.82	0.78
11	0.13	0.09	0.07	0.41	0.58
12	0.38	0.04	0.09	0.35	0.44
13	0.75	0.13	0.15	0.35	0.36
14	0.75	0.43	0.39	0.24	0.28
15	0.38	0.35	0.37	0.24	0.11
16	0	0.04	0.13	0.12	0

TABLE IV. Visible and UV bands recorded in the emission spectrum. Operating conditions were: P_{He} = 3.87 torr, P_{O_2} = 0.60 torr, $P_{C_3O_2}$ = 0.19 torr, and a 12 Kv discharge. The reported wavelengths are estimates of the band maxima, whereas entries under λ_{true} are band heads as given by Pearse and Gaydon, "The Identification of Molecular Spectra", John Wiley and Sons, Inc., New York (1963). The O_2 bands are double-headed under higher resolution.

λ_{obs} (Å)	I_{obs}	Emitter	λ_{true} (Å)	Assignment (v'-v'')	System
5898	24	C_2	5899.3	6-8	high pressure
5635	24	C_2	5635.5	0-1	Swan
5584	24	C_2	5855.5	1-2	"
5541	36	C_2	5540.7	2-3	"
5502	23	C_2	5501.9	3-4	"
5469	22	C_2	5470.3	4-5	"
5432	26	C_2	5434.9	6-7	high pressure
5163	82	C_2	5165.2	0-0	Swan
5128	59	C_2	5129.3	1-1	"
5097	40	C_2	5097.7	2-2	"
4736	49	C_2	4737.1	1-0	"
4714	78	C_2	4715.2	2-1	"
4696	65	C_2	4697.6	3-2	"
4676	100	C_2	4678.6	5-4	"
4365	47	C_2	4365.2	4-2	"
3852	8	C_2	3852.2	0-0	Deslandres-d'Azambuja
3690	5	CO_2	3691.8		Fox, Duffendack and Barker
3620	2	CO_2	3621.0		"
3607	5	C_2	3607.3	1-0	Deslandres-d'Azambuja
3369	0.6	CO_2	3370.0		Fox, Duffendack and Barker
3296	0.7	O_2^+	3322.6 3300.3	1-5	second negative
3125	0.4	O_2^+	3141.0 3123.1	1-4	"

2968	0.5	O_2^+	2987.5 2970.0	3–4	Second negative
2828	0.6	O_2^+	2839.7 2823.7	3–3	"
2661	0.7	O_2^+	2666.5 2652.3	6–3	"
2589	0.6	O_2^+	2594.3 2581.0	5–2	"
2536	0.8	O_2^+	2532.8 2512.9	6–2	"
2478	0.6	O_2^+	2478.0 2465.8	5–1	"
2447	0.4	O_2^+	2458.6 2446.9	8–2	"
2420	0.4	O_2^+	2433.5 2421.8	6–1	"
2385	0.5	O_2^+	2392.6 2381.0	8–1	"

FIGURE 1a,b,c.   Schematics for Reactor.   Parts designated with lower case letters are stationary; those with capitals rotate at about 2 cps.

a.   He inlet tube on right; He + C_3O_2 outlet tube on left

b.   Clamp for scraper and inlet/outlet structure

c.   Supporting tube

d.   Support for bearing

e.   He + C_3O_2 collecting tube

f.   Cover for tape heater

g.   Tape heater – current controlled by variac

h.   Scraper

i.   He inlet tube

j.   motor

ℓ.   Bearing for rotating structure

m.   Gear box

A.   End plates

B.   Glass tube

C.   Spacer rods

D.   Gear

K.   Rotating bushing – attached to gear and end plate
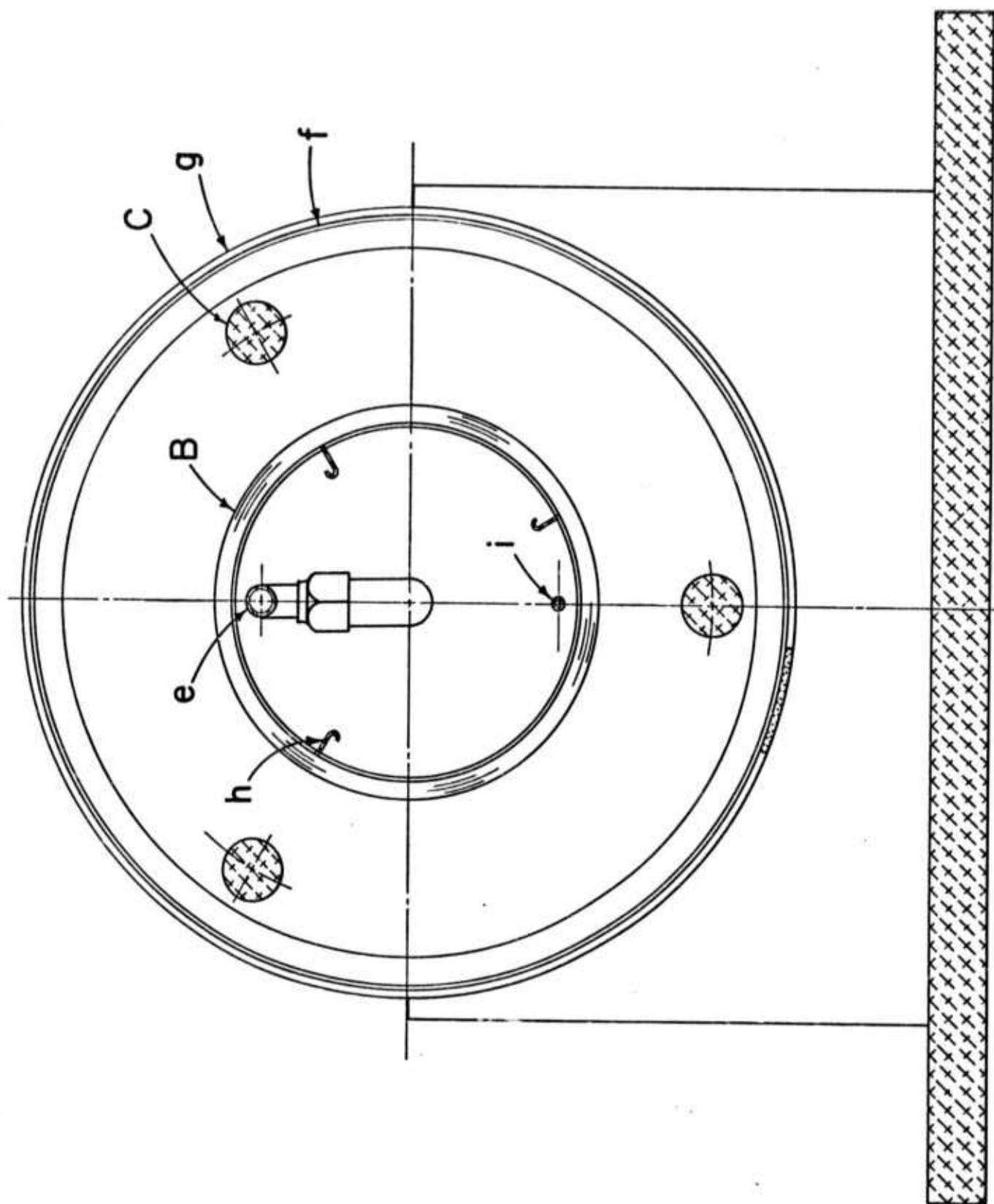
Front Section

Fig. 5

Fig. 1a

Top View

55-
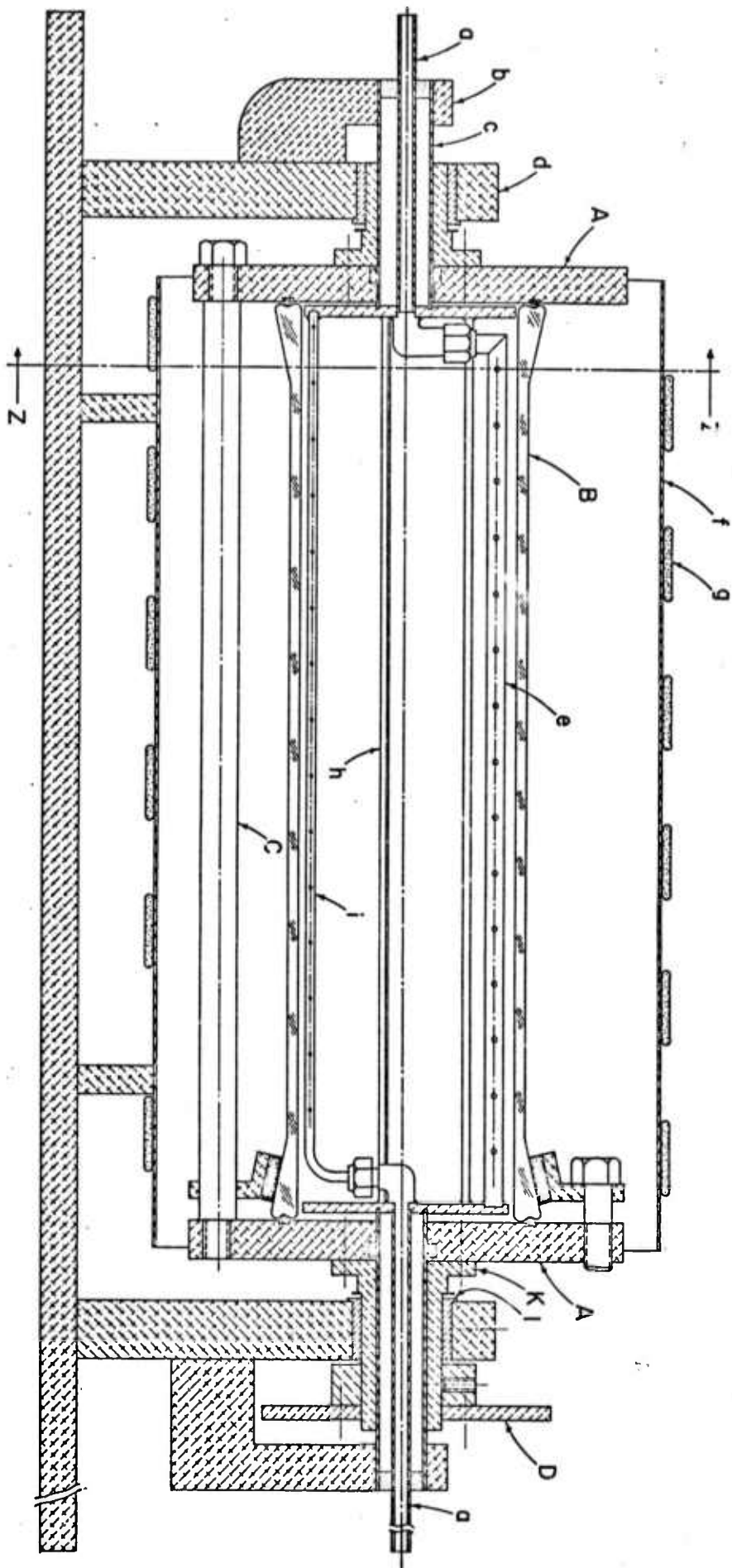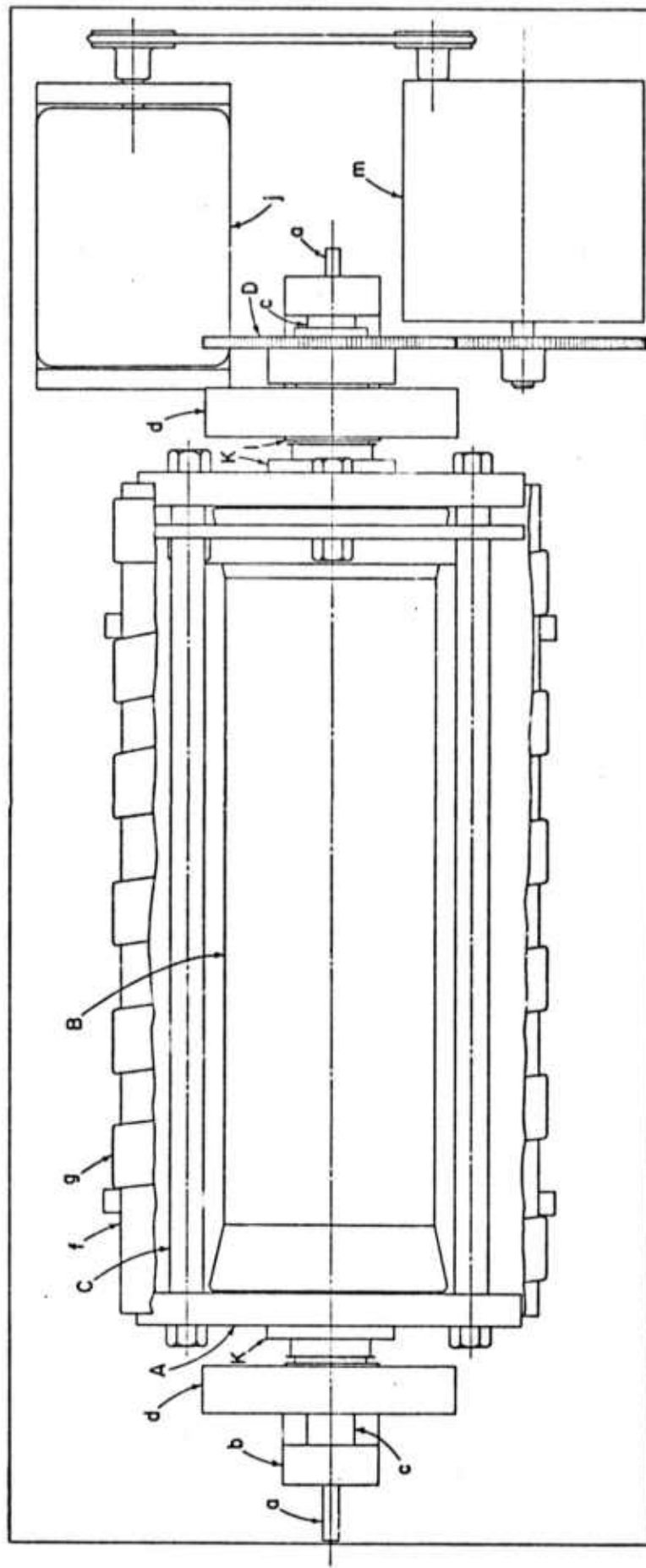
Section Z-Z

Fig 1c

FIGURE 3.   Integrated power dependence on C_3O_2 pressure.

P_{He} = 3.75 torr P_{O_2} = 0.62 torr

Discharge Voltage (Kv)	$P_{C_3O_2}$ =	Power (arbitrary units)		
		0.15 torr	0.20 torr	0.28 torr
9		4.8	2.0	-
10		10.4	28.0	5.0
11		9.4	47.0	10.0
12		4.6	44.0	25.0
13		0.6	26.0	40.0
14		0.3	11.0	44.0
15		-	2.0	30.0

malonic acid + P_2O_5

heating mantel

liquid N_2

liquid N_2

Hg manometer

to pump
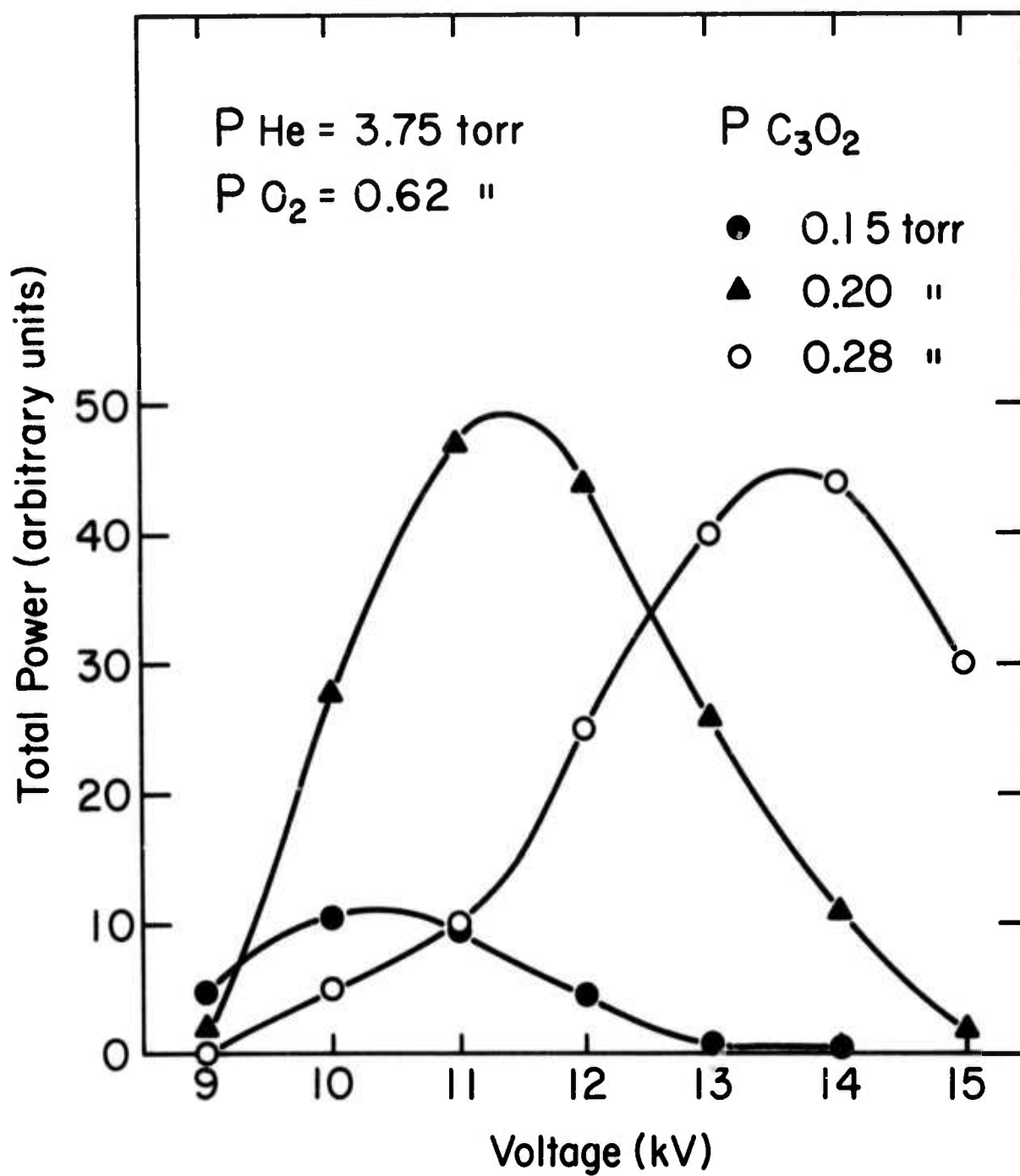
transfer to storage trap

liquid N_2

Fig 2

58 cm
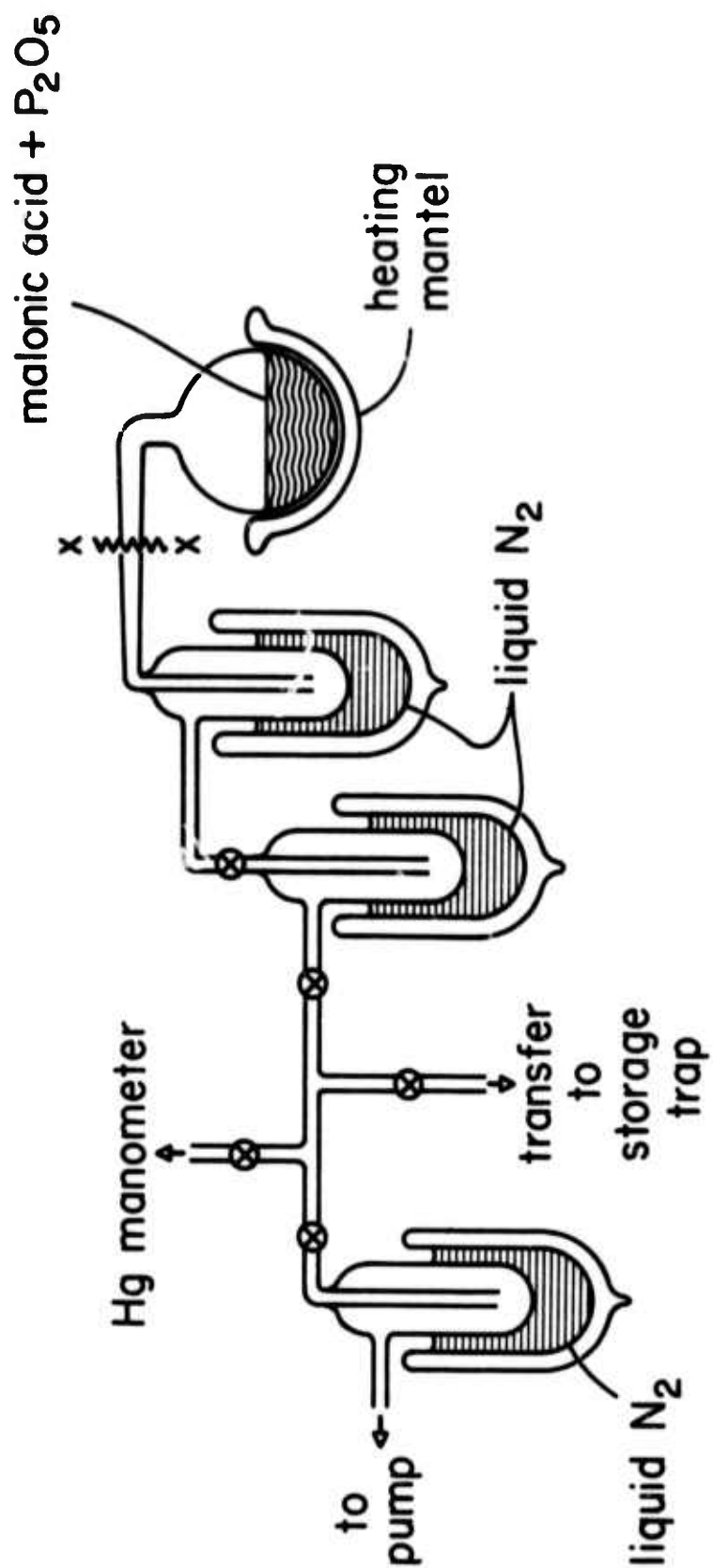
FIGURE 2.   Schematic diagram for the preparation of C_3O_2: Static reactor.

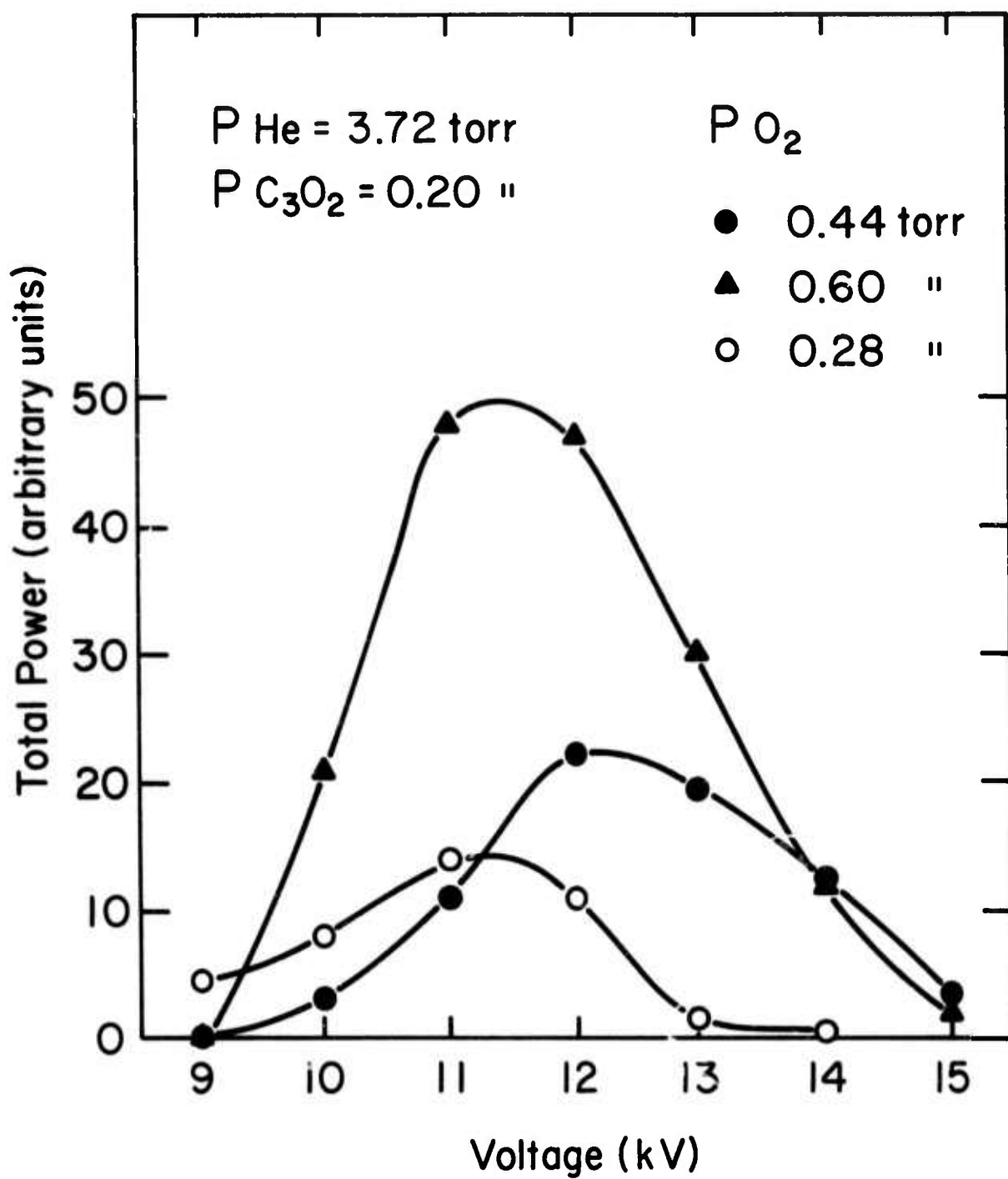The output from the rotating reactor (Fig. 1) was fed into the

purification train at x—x.

59

60

FIGURE 4.   Integrated power dependence on O_2 pressure.

$$P_{He} = 3.72 \text{ torr} \qquad P_{C_3O_2} = 0.20 \text{ torr}$$

Discharge Voltage (Kv)	$P_{O_2} =$	Power (arbitrary units)		
		0.44 torr	0.60 torr	0.95 torr
9		-	-	4.5
10		3.0	21.0	8.0
11		11.0	48.0	14.0
12		22.0	47.0	11.0
13		19.5	30.0	1.6
14		12.5	12.0	0.5
15		3.5	2.0	-

P He = 3.72 torr
P C_3O_2 = 0.20 "

P O_2

- 0.44 torr
▲ 0.60 "
○ 0.28 "

Total Power (arbitrary units)

Voltage (kV)

62

FIGURE 5.   Integrated power dependence on He pressure.

$$P_{O_2} = 0.60 \text{ torr} \qquad\qquad P_{C_3O_2} = 0.20 \text{ torr}$$

Discharge Voltage (Kv)	$P_{He} =$	Power (arbitrary units)		
		2.48 torr	3.72 torr	5.57 torr
9		4.0	-	-
10		9.5	21.0	38.0
11		24.0	48.0	67.0
12		22.0	47.0	55.0
13		12.5	30.0	30.0
14		4.5	12.0	8.5
15		0.0	2.0	0.6

64-

FIG 5
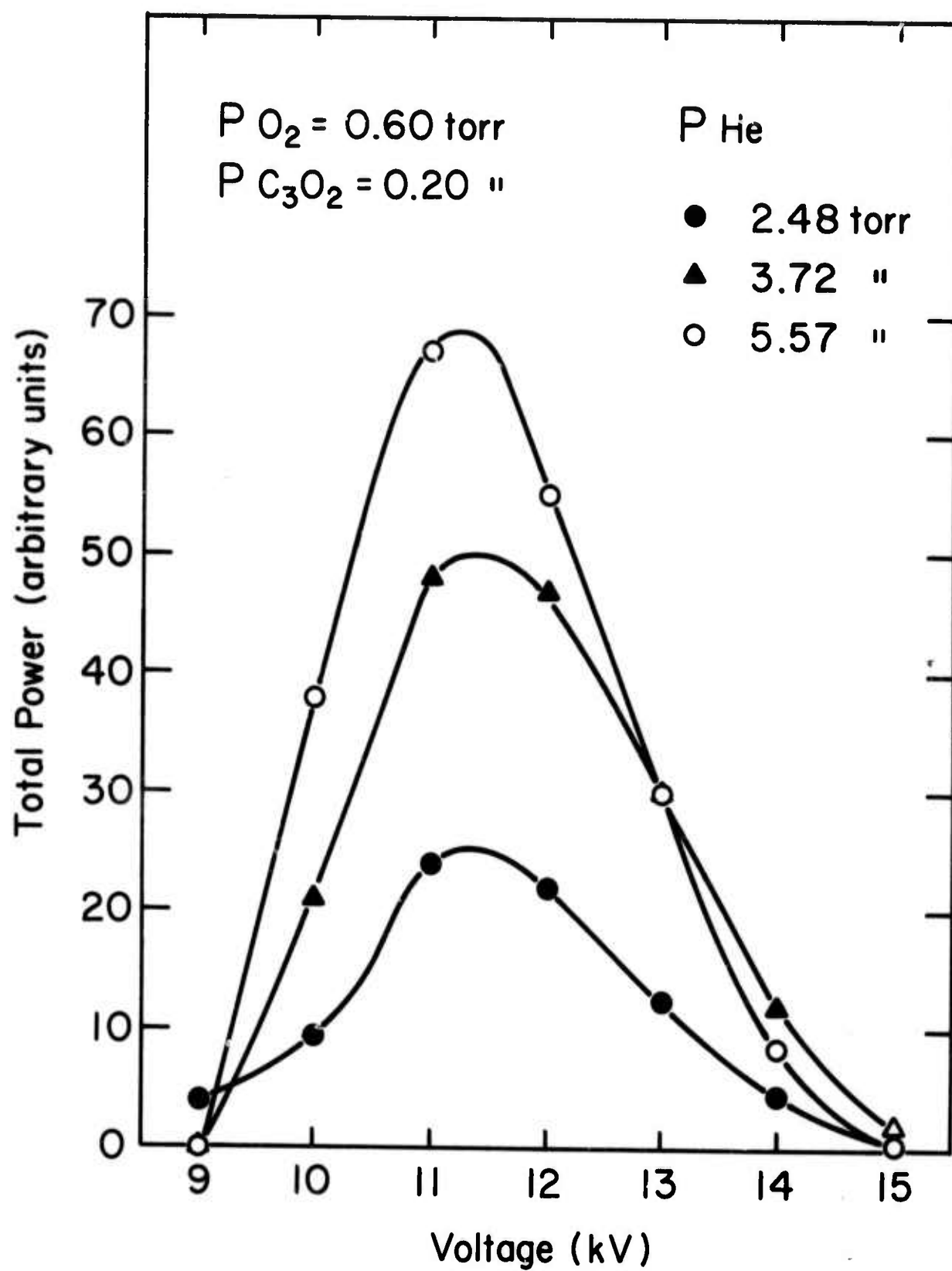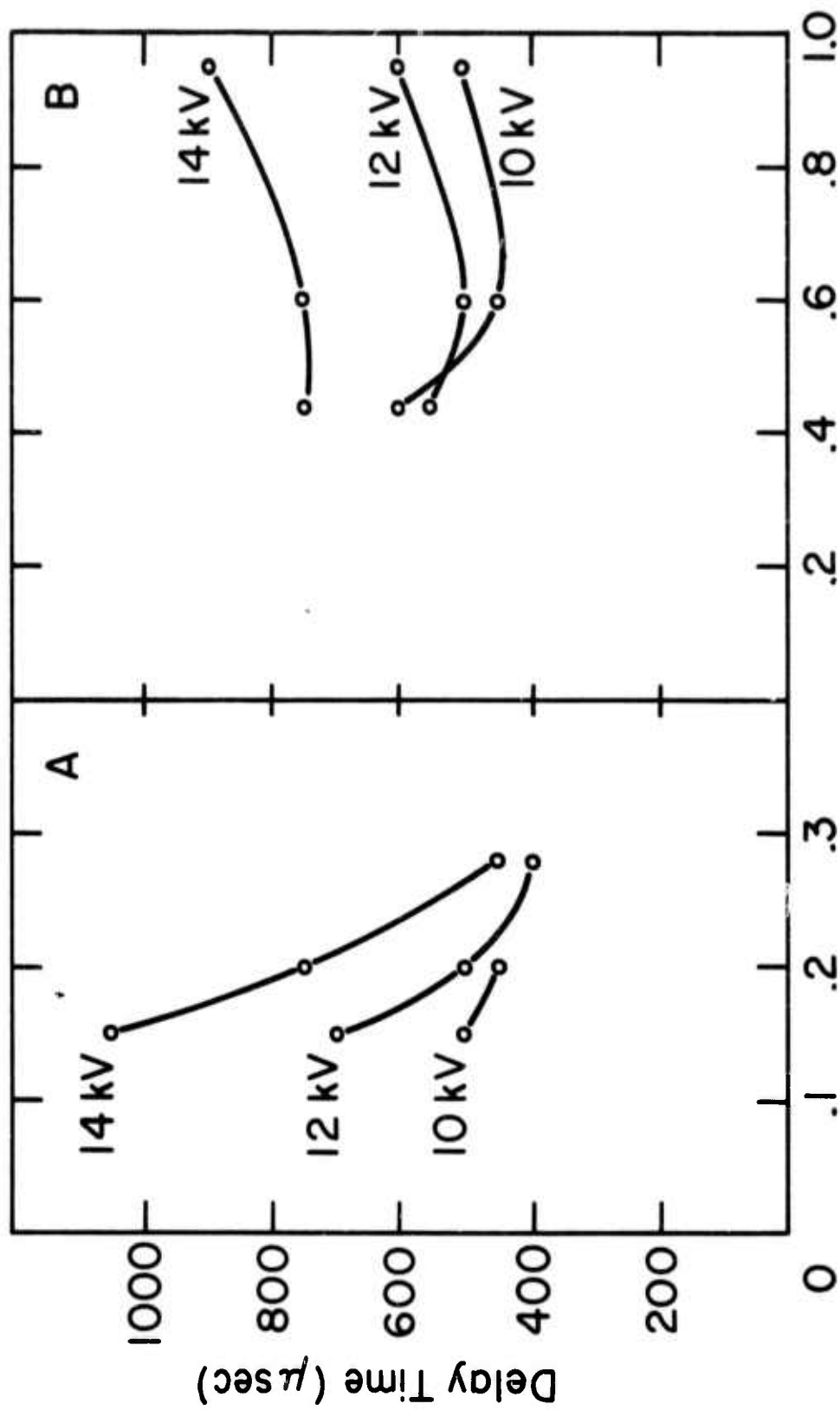
FIGURE 6.   Dependence of delay times on operating conditions.

Part (a) P_{He} = 3.72 torr P_{O_2} = 0.60 torr

Discharge Voltage (Kv)	$P_{C_3O_2}$ =	Delay time (μsec)		
		0.15 torr	0.20 torr	0.28 torr
10		500	450	-
12		700	500	400
14		1050	750	450

Part (b) P_{He} = 3.72 torr $P_{C_3O_2}$ = 0.20 torr

Discharge Voltage (Kv)	P_{O_2} =	Delay time (μsec)		
		0.44 torr	0.60 torr	0.95 torr
10		600	450	500
12		550	500	600
14		750	750	900

65

Fig. 6

$P O_2$ (torr)

$P_{He} = 3.72$ torr
$P_{C_3O_2} = 0.20$ "

$P_{C_3O_2}$ (torr)

$P_{He} = 3.72$ torr
$P_{O_2} = 0.60$ "

FIGURE 7.   Integrated power dependence on the pressure of added CO.

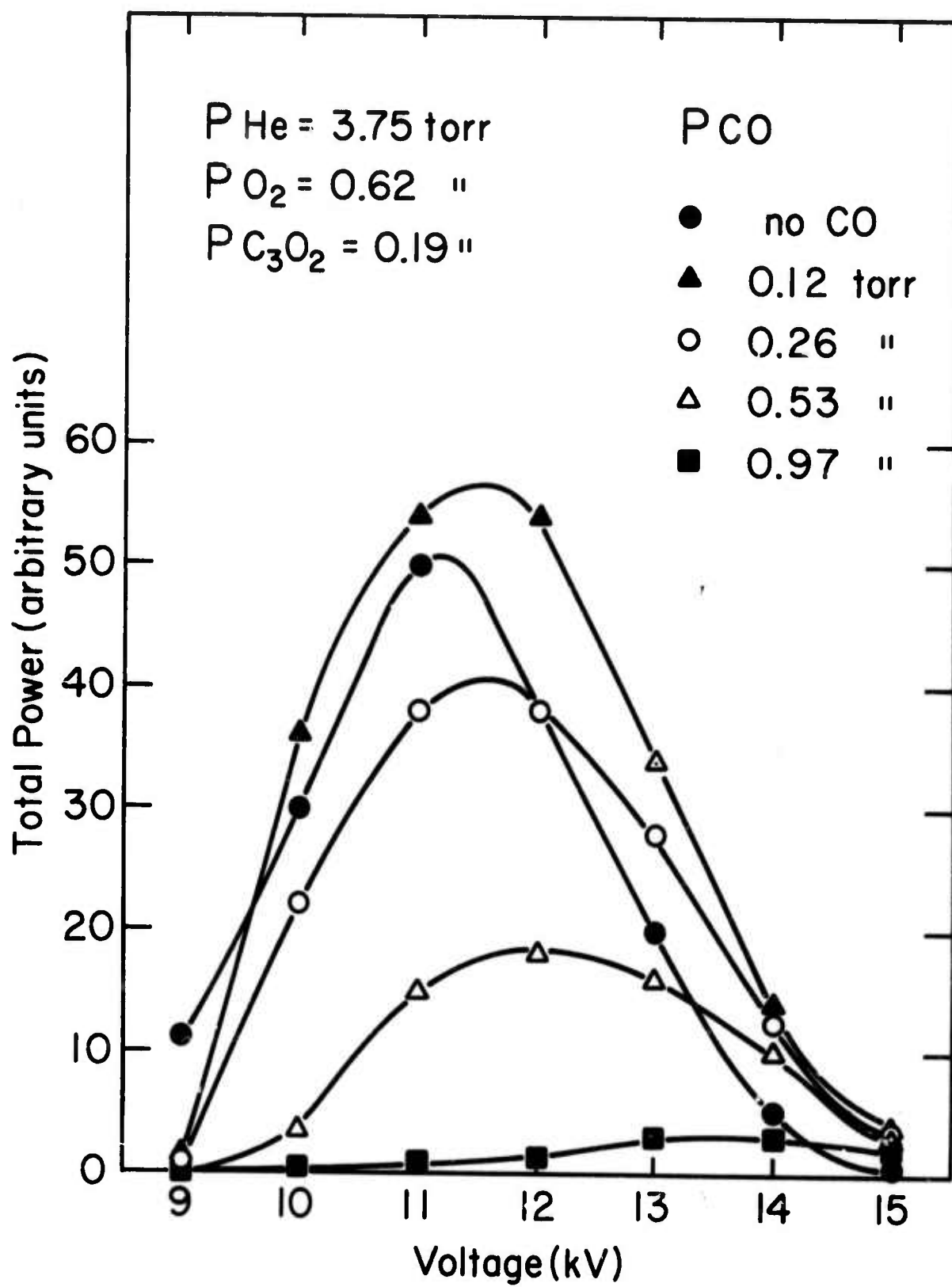P_{He} = 3.75 torr P_{O_2} = 0.62 torr $P_{C_3O_2}$ = 0.19 torr

Power (arbitrary units)

Discharge Voltage	NO CO	P_{CO} (torr)			
		0.12	0.26	0.53	0.97
9	11.0	1.0	0.8	–	–
10	30.0	36.0	22.0	3.5	0.2
11	50.0	54.0	38.0	15.0	1.0
12	38.0	54.0	38.0	18.0	1.2
13	20.0	34.0	28.0	16.0	3.0
14	5.0	14.0	15.0	10.0	3.1
15	0.8	4.0	3.6	3.0	2.2

P He = 3.75 torr
P O_2 = 0.62 "
P C_3O_2 = 0.19 "

Pco
●   no CO
▲   0.12 torr
○   0.26   "
△   0.53   "
■   0.97   "

68—

FIG 7

FIGURE 8.   Dependence of delay times on the pressure of added CO.

$$P_{He} = 3.75 \text{ torr} \qquad P_{O_2} = 0.62 \text{ torr} \qquad P_{C_3O_2} = 0.19 \text{ torr}$$

Delay time (μsec)

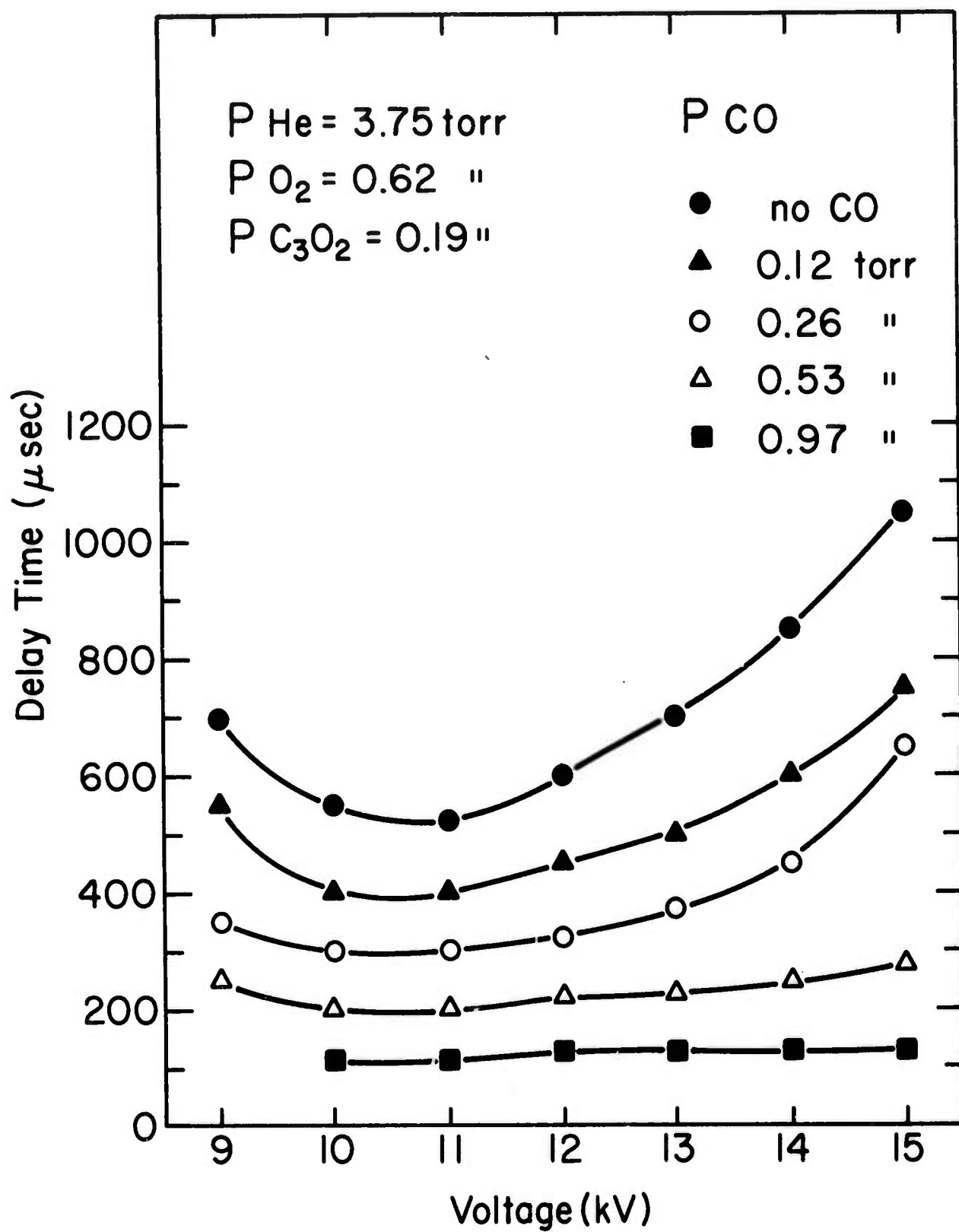| Discharge Voltage (Kv)	NO CO	P_{CO} (torr)			
		0.12	0.26	0.53	0.97
9	700	550	350	250	-
10	550	400	300	200	110
11	525	400	300	200	110
12	600	450	325	225	125
13	700	500	375	225	125
14	850	600	450	250	130
15	1050	750	650	275	130

FIG 8

FIGURE 9.   Relative vibrational populations of CO at selected time delays.

The distributions have been normalized at v = 8.

NOTE: There are both theoretical and experimental indications
that the distribution given for 100 μs is in error. Please
disregard this curve.

72—

Fig 9
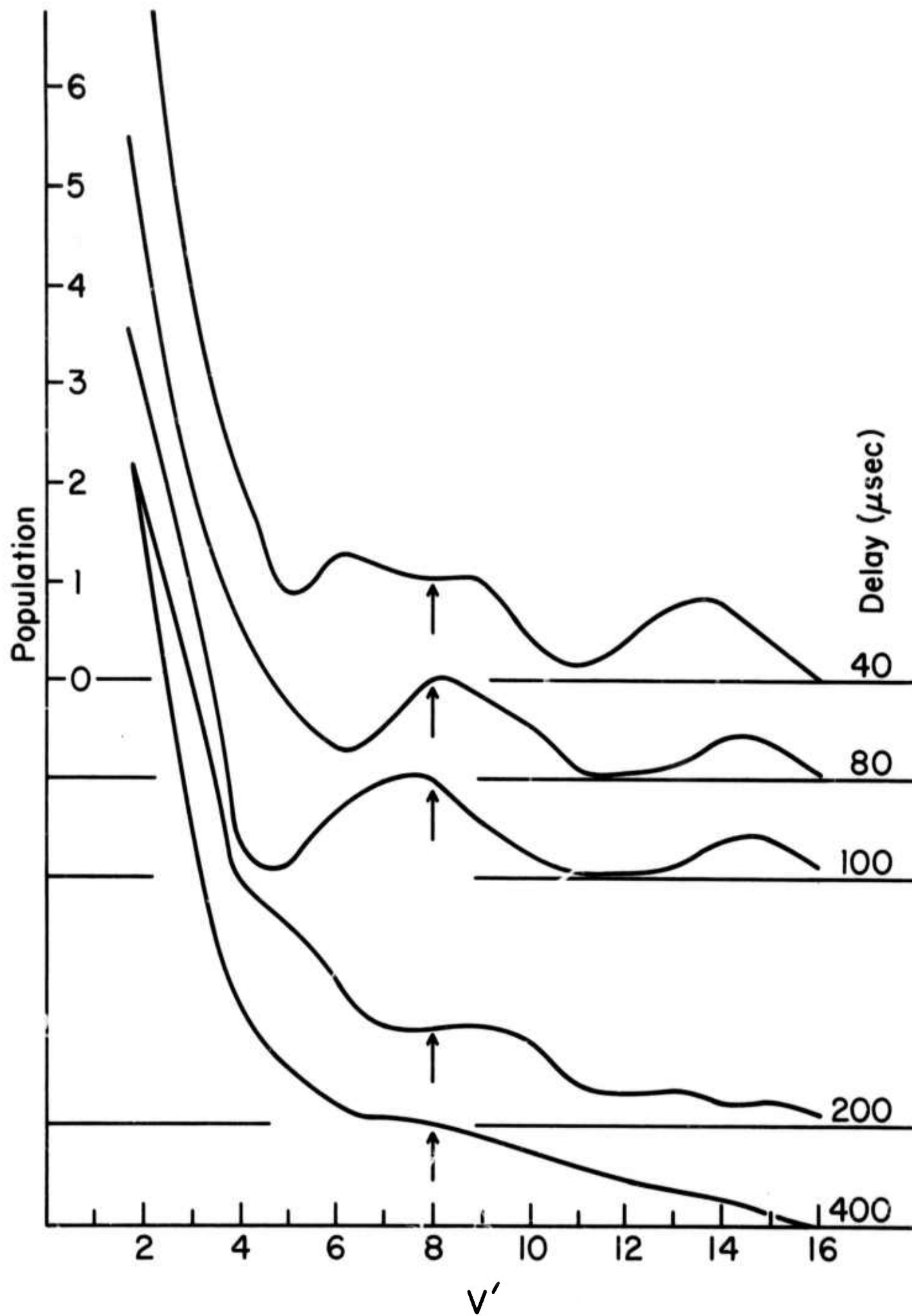
4.   MOLECULAR RELAXATION VIA COLLISIONS WITH ATOMS

Professor G. J. Wolga and R. A. McFarlane

A.   Introduction

Two complete experimental facilities were put into operation during the past contract year to measure the rate of molecular vibrational relaxation upon collision with atoms. Such rates have not previously been studied at the low temperatures appropriate to efficient laser operation for most molecules of interest. This is because conventional methods e. g. : shock tube relaxation studies, require high temperatures for the thermal production of atoms. Such rates, however, are very important for accurate modeling of laser performance whenever gas discharges, electron beams, or chemical reactions are employed for laser pumping since, under such circumstances, many atoms are present. In addition to the practical significance for laser modeling, knowledge of such rates is important to the theoretical understanding of vibrational relaxation since an atom-molecule collision is a relatively simple three center collision system which may prove amenable to accurate calculations. For example, recent work of Nikitin[1] emphasizes the importance to molecular vibrational relaxation of a collision in which the collider possesses orbital degeneracy. Thus, deactivation by F, Cl, and O apply to this theory while deactivation by H and N do not.

The experimental facilities utilize the laser induced fluorescence method to excite molecular vibrational energy by the absorption of a resonant photon and to monitor the relaxation by the ensuing fluorescence. Absolute atom concentrations are measured using electron microwave paramagnetic resonance with calibration by the absorption by

$O_2(^3\Sigma_g^-)$ according to methods developed by Westenberg[2]. This technique is quite universal and permits measurement of any molecule that can be optically pumped from the ground vibrational state and any atom possessing an electronic magnetic moment. Both experimental facilities use a TEA laser to provide resonant laser emission and a fast flow system in which atoms are produced upstream by microwave dissociation. The molecule to be studied is mixed into the flow downstream and the atom-molecule mixture with diluent undergoes laser induced fluorescence in an optical cell and atom concentration determination farther downstream. Atom concentration decay by wall and volume recombination are measured for the flow tube employed to permit calibration of the atom concentration in the fluorescence cell from a measurement made somewhat farther downstream. Fluorescence measurements are made with and without the microwave discharge (atom production) to permit the effect of the atoms to be isolated. The fluorescence decay curves are signal averaged for improved precision. The typical apparatus is schematically illustrated in Figures 1 and 2.

B.   HF/DF Relaxation via Atom Collisions

Our program was to measure the relaxation of HF(v = 1) and DF(v = 1) due to collisions with H, D, F, N, O. We employ a TEA excited HF chemical laser optimized for v = 1 → O transitions. Because of the very fast self relaxation of HF it is important to optimize the atom production and to achieve fast flow so as to have a large atom concentration for a measurable change in the HF/DF decay rate. The results we have obtained to date are:

$$(p\tau)^{-1}_{HF(1):H} \leq 10^4 \ sec^{-1} \ Torr^{-1} \quad ; \quad T = 300 \ K$$

$$(p\tau)^{-1}_{HF(1):F} = 1.2 \times 10^4 \ sec^{-1} \ Torr^{-1}; \quad T = 300 \ K$$

Experiments are in progress to complete the HF(1):H rate determination after which deactivation by D, N, and O will be studied followed by similar studies on DF(v = 1). We expect this work to be completed during February, 1974, after which we shall study other alkali halide molecules.

75—

C. $\underline{CO_2(00{}^{\bullet}1) \text{ Relaxation via Atomic Collisions}}$

Our program was to measure the relaxation of $CO_2(00{}^{\bullet}1)$ due to collisions with H, D, F, N, O. We employ a TEA CO_2 laser at 10.5 microns to populate the $(00{}^{\bullet}1)$ state. Measurements with CO_2 are difficult because of the relatively slow self relaxation and, with the exception of H and O, the relatively slow decay due to atom collisions. Thus, only small collisional effects are observed during the molecular residence time in the fluorescence cell. The results we have obtained to date are:

$$(p\tau)^{-1}_{CO_2(00{}^{\bullet}1):O} = 1.1 \times 10^4 \text{ sec}^{-1} \text{ Torr}^{-1} \quad , \quad T = 300 \text{ K}$$

$$(p\tau)^{-1}_{CO_2(00{}^{\bullet}1):N} \leq 2.2 \times 10^3 \text{ sec}^{-1} \text{ Torr}^{-1} \quad , \quad T = 300 \text{ K}$$

$$(p\tau)^{-1}_{CO_2(00{}^{\bullet}1)-H} = 1.7 \times 10^4 \text{ sec}^{-1} \text{ Torr}^{-1} \quad , \quad T = 300 \text{ K}$$

Additional results obtained in conjunction with the above determinations are:

$$(p\tau)^{-1}_{N_2(v=1):O} \leq 2.6 \times 10^3 \text{ sec}^{-1} \text{ Torr}^{-1} \quad , \quad T = 300 \text{ K}$$

$$(p\tau)^{-1}_{CO_2(00{}^{\bullet}1):H_2} = 3.8 \times 10^3 \text{ sec}^{-1} \text{ Torr}^{-1} \quad , \quad T = 300 \text{ K}$$

We anticipate completing relaxation studies using F and D atoms in the near future.

D. CO(v = 1) Relaxation via Atomic Collisions

Another apparatus is nearing completion for studies of CO relaxation resulting from collisions with atoms. We have completed design and construction of a frequency doubled CO_2 TEA laser using phase matched single crystal Tellurium as the nonlinear crystal. The TEA laser is diffraction grating controlled for single line operation with a tunable etalon available for further wavelength control. With this source we shall pump CO to the v = 1 state. Our first relaxation work will study the effect of O atoms using gas titration methods to obtain O atom concentrations. However, a paramagnetic resonance spectrometer will be available for study of other atoms during the next contract year.

References

1.   E. E. Nikitin and S. Ya' Umanski, Comments on Atomic and
        Molecular Physics, Vol. 3, No. 6, Nov. - Dec., 1972.

2.   A. A. Westenberg, Prog. in Reaction Kinetics, $\underline{7}$, Part I (1973),
        Pergamon Press.

78-

For some time we have been studying the effect of vibrational
excitation of $HF(v)$ upon the rate constant for the four center atom
exchange reaction

$$HF(v) + D_2 \xrightarrow{\quad k_v \quad} HD + DF$$
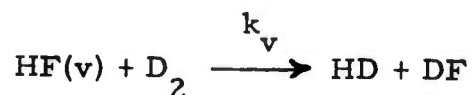
Prior work[1, 2] on the analogous reactions

$$H_2 + D_2 \rightarrow 2HD$$

$$HCl + D_2 \rightarrow HD + DCl$$
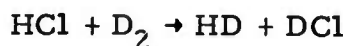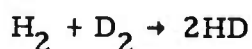
indicated that to explain the production of HD at the experimental conditions
employed required a mechanism involving the vibrational excitation of
at least one of the reactants. In the early $H_2 + D_2$ studies[3] and in the
$HCl + D_2$ reaction shock tubes were employed and a broad temperature
range ensued during the experiment. In the most recent study of the
$H_2 + D_2$ reaction[1] H_2 was pumped to the $v = 1$ state and subsequent V-V
pumping was assumed to bring H_2 to a sufficiently high vibrational level
for the reaction to occur. We undertook the study of $HF(v) + D_2$ because
direct vibrational excitation of HF to specific vibrational levels by absorption
of resonant HF laser radiation could be specified and controlled. It was
felt that this important prototype reaction could be best studied in this way.
A significant enhancement of the rate of chemical reaction that was shown
to depend upon vibrational excitation of a hydrogen halide reactant would
have possibly important bearing upon the performance of high power HF
chemical lasers which contain precisely the reactants we are studying,
$HF(v)$ and H_2 (D_2 in our experiment). This atom exchange reaction could
provide a vibrational energy loss mechanism for the laser since it is

possible, but as yet unproven, that the vibrational excitation is degraded in the reaction.

The method we employ consists of irradiating a sample of $HF + D_2$ with a time sequence of HF laser radiation chosen to successively pump HF in the sequence $\Delta v = 0 \to 1, 1 \to 2, 2 \to 3$. An identical companion cell is filled to the same partial pressures and held at the same temperature. The sample cell is irradiated a chosen number of times after which mass spectrometric determination of sample and reference cell concentrations is made. This analysis yields the relative changes of HD concentration

$$\Delta(HD)/D_2 \text{ defined as } (HD)_{sample} - (HD)_{reference}/(D_2).$$

We have also estimated a maximum temperature rise to be associated with each irradiation as $100\,^{\circ}C$ for 10^{-3} sec. To determine the likelihood of HD production during this period of increased temperature we performed additional experiments with the sample held at temperatures within the range $350 - 450\,^{\circ}C$ for 30 minutes. Mass spectrometric analysis showed no significant HD production due to thermal excitation at the temperatures studied. We therefore conclude that thermal effects are negligible in our experiments.

Our results to date are:

1.   A very significant enhancement of HD production is observed as a result of laser vibrational pumping.

2.   Excitation by laser pumping to $v = 3$ is required. Excitation to lower vibrational levels followed by V-V energy exchange does not lead to significant HD production.

3. HD production is measurable with good signal to noise. Thus a quantitative determination of the rate constant will be possible.

4. A simple analysis of HD production based on the phenomenological rate equation

$$\frac{d[HD]}{dt} = k_{v=3}[HF(v=3)][D_2]$$

has been made. Our initial assumption as to the population of $HF(v=3)$ at $t=0$ assumes that optical saturation occurs in the successive absorptions. We insert the V-V deactivation rate of $v=3$ as measured by Osgood to integrate this equation under the assumption that only $HF(v=3)$ is involved in the reaction. We can thus solve for $k_{v=3}$ using the known parameters $\Delta(HD)/D_2$. The result is $k_{v=3} \approx 1.2 \times 10^{11}$ cm^3/mole-sec. This result fits an Arrhenius form for the rate constant $k_3 = A \exp{-[E_0 - E_3]/RT}$ with $A \approx 10^{13}$ and $E_0 \approx 38\text{-}39\,kcal/mole$ which agrees well with the earlier results on the $H_2 + D_2$ and $HCl + D_2$ reactions.

We are currently involved in spectroscopic studies aimed at elucidating the mechanism for the reaction. By very carefully specifying the conditions under which optimum conversion occurs we hope to verify the vibrational excitation mechanism. After we optimize the conversion we shall seek to determine whether this reaction is of importance in HF lasers.

References

1. D. M. Lederman and S. H. Bauer, Int. Jn. of Chem. Kinetics, 5, 93 (1973).

2. R. D. Kern and G. G. Nika, J. Phys. Chem., 75, 171 (1971).

3. S. H. Bauer and E. L. Resler, Jr. Science, 146, 1045 (1964).

82—